2-8-2011

The Nature and Kinetic Analysis of Carbon-Carbon Bond Fragmentation Reactions of Cation Radicals Derived from SET-Oxidation of Lignin Model Compounds

Adam Pimentel

Adam S. Pimentel
Candidate

Chemistry and Chemical Biology
Department

This thesis is approved, and it is acceptable in quality and form for publication:

Approved by the Thesis Committee:

Debra Dunn-Mascetta, Chairperson

The Nature and Kinetic Analysis of Carbon-Carbon Bond Fragmentation Reactions of Cation Radicals Derived from SET Oxidation of Lignin Model Compounds.

BY

ADAM S. PIMENTEL

B.S. Chemistry, B.A. Mathematics
University Of North Carolina at Asheville, 2001

THESIS

Submitted in Partial Fulfillment of the
Requirements for the Degree of

Master of Science
Chemistry and Chemical Biology

The University of New Mexico
Albuquerque, New Mexico

December, 2010

DEDICATION

To my wife and daughter,
Jill Ann Lingenfelter and Elaine Kathryn Pimentel

ACKNOWLEDGEMENTS

I would like to express my sincere gratitude to Dr. Debra Dunaway-Mariano and Dr. Patrick S. Mariano for their guidance, encouragement and not least for their patience in the production of this work. I would like to thank Dr. Wei Wang for agreeing to be a member of my advisory board.

I would like to extend my sincere appreciation to Dr. Dae Won Cho for his additional guidance and many hours of discussion and advice, which were instrumental to any success that I can claim.

I wish to acknowledge the valuable contributions of the current and former members of the Dunaway-Mariano and Mariano groups for their helpful support and friendship. In particular Dr. Zhimin Li, Dr. Jian Cao, Hong Zhao, Danqui Chen, Hua Huang and Min Wang for their kindness, generous advice, and tireless answers to countless questions. Thanks also to Gabriel Maestes for his friendship, camaraderie, and indomitable and infectious spirit.

It is my great pleasure to acknowledge the love and support of my family, in particular my wife, Jill Lingenfelter and daughter Elaine Pimentel, as well my parents-in-law, Bob and Elaine Lingenfelter for their enduring belief and support, and also, not least, their patience as well.

The Nature and Kinetic Analysis of Carbon-Carbon Bond Fragmentation Reactions of Cation Radicals Derived from SET Oxidation of Lignin Model Compounds.

BY

ADAM S. PIMENTEL

ABSTRACT OF THESIS

Submitted in Partial Fulfillment of the
Requirements for the Degree of

Master of Science
Chemistry and Chemical Biology

The University of New Mexico
Albuquerque, New Mexico

December, 2010

THE NATURE AND KINETIC ANALYSIS OF CARBON-CARBON BOND FRAGMENTATION REACTIONS OF CATION RADICALS DERIVED FROM SET-OXIDATION OF LIGNIN MODEL COMPOUNDS

by

Adam S. Pimentel

B.S. Chemistry, B.A. Mathematics, University of North Carolina, Asheville, 2001

M.S. University of New Mexico, 2010

ABSTRACT

The lignin peroxidase promoted α–carbon β–carbon bond cleavage of two diastereomeric pairs of dimeric lignin model compounds were investigated to determine which structural units are more readily cleaved. These model compounds, β-1 (1,2-diaryl-1,3-propanediol) and β-O-4 (1-diaryl-2-aryloxy-1,3-propanediol), represent the most common structural units present in the plant cell wall polymer lignin. The lignin peroxidase catalyzed reaction mechanism was shown to parallel two mechanistically well understood systems, the cerric (IV) ammonium nitrate promoted chemical reacton, and the dicyannoanthracene promoted photochemical reaction, both of which proceed by a SET mechanism. Product profiles and kinetic rate constants were determined and compared for all four model compounds by HPLC and Stopped Flow kinetic techniques.

TABLE OF CONTENTS

LIST OF FIGURES

LIST OF SCHEMES

LIST OF TABLES

Introduction

The goal of my Masters Degree research work was to probe the lignin peroxidase promoted carbon-1 carbon-2 cleavage reactions of two diastereomeric pairs of dimeric lignin model compounds. The model compounds represent the common structural units found in the heterogeneous plant cell wall polymer lignin.[1] These structural units are termed β-1 (1,2-diaryl-1,3-propanediol) and β-O-4 (1-diaryl-2-aryloxy-1,3-propanediol). The studies are aimed at gaining an understanding of the basic chemistry underlying lignin breakdown promoted by a fungus derived enzyme known as lignin peroxidase (LP). The goal of the work is to determine which structural units in lignin are more readily cleaved by LP. In the long run, the results could serve as a foundation of a wider investigation the establish methods for predicting strategies for genetic manipulation of biomass sources to produce plants that contain more readily enzymatically degradable lignin and, thus, more easily accessible cellulose.

Background

Ethanol as a Biofuel. Current sources of plant-derived ethanol consist primarily of starch containing crops such as corn. The starches in these plants are converted by a cocktail of hydrolytic enzymes to glucose, which is then subjected to fermentation to produce ethanol. The main problem with this approach to biofuel production is that it relies on edible starch bearing crops and, as such, ethanol production competes with use as a food source.[2]

Recently, much interest has been generated in the possibility of using alternate, non-food based plants as sources of ethanol. These plants are wide spread and include grasses and straws, wood, lumber industry or agricultural wastes (*eg.,* spent paper pulp and processed crop residues) and municipal waste. A DOE sponsored study by Wang and others showed that implementation of biomass ethanol in lieu of gasoline could reduce greenhouse gas emissions by up to 86 %.[3]

The goal of developing processes to convert plant materials into ethanol in an efficient and cost effective manner is confronted by several key obstacles. However, advances are being made and, in fact, one of the worlds largest industrial enzyme providers recently announced the creation of a low cost suite of cellulase enzymes, which transform celluose to ethanol. It is projected that this finding will bring the cost of cellulosic ethanol to below $2.00 per gallon.[4] Additionally, a strain of E. coli has been produced that can ferment xylose, a primary component of the other predominant plant cell wall polysaccharide mixture known as hemicellulose.[5]

Advances in cellulosic enzymology and bacteriology over the last two years has reduced the cost of biomass derived ethanol by 80 %, and further advances in process technology combined with continued biological improvements are expected to further reduce the cost of cellulosic ethanol production.[5] For

example, substitution of chemical pretreatment with enzymatic degradation of plant materials to liberate cellulose and other plant polysaccharides could lead to more efficient production of glucose and, as a result, reduce the cost of biomass-derived ethanol. Pretreatment of plant materials is required in order to degrade the heterogeneous polymer lignin which encapsulates the sugars and prevent their ready hydrolysis to form glucose.[6]

Plant Cell Walls. The discussion of biomass as a fuel source begins with a consideration of what biomass is and where it comes from. All of the key plant polymers are contained within the cell walls of plants, which is composed of the middle lammela, a border joining contiguous cells, a primary wall and three distinct secondary walls. The cell wall plays a vital role in the survival of the plant by assisting in nutritive uptake, the transport and secretion of various substances for nutrition and defense, and as structural support.[7] The contents of the cell wall of primary interest in biofuel production are cellulose, hemicellulose, and lignin (Figure 1).

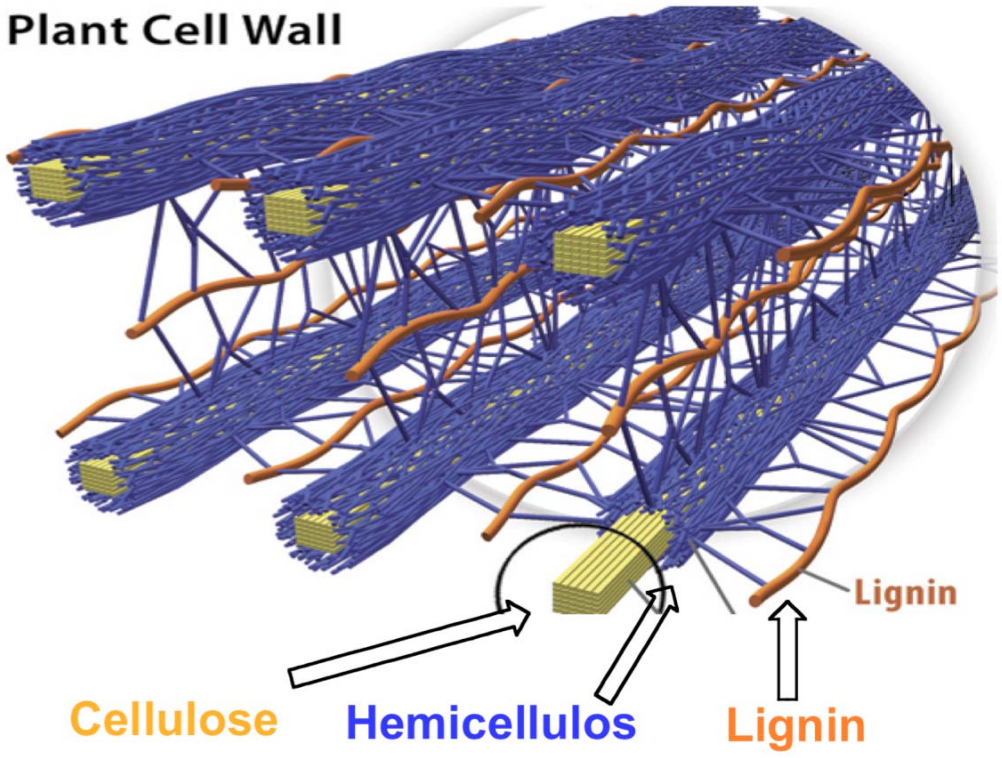

Figure 1. *Depiction of the plant cell wall.*

Cellulose is a polysaccharide consisting of a regular chain of glucose units linked by β-1,4 glycosidic bonds. These β-1,4 linkages render the resulting cellulose indigestible to mammals that can easily digest the similar α-1,4 glycosidic linkages present in many starch containing food sources. Importantly, cellulose makes up 40-45% of dried plant materials. Hemicellulose, a more highly branched polysaccharide, is also present in plant cell walls where it contributes to 20-30% of the weight of dried plants. Hemicellulose is an amorphous substance of average molecular weight 200-300 and is primarily composed of D-glucose, D-mannose, D-galactose, D-xylose and L-arabinose units.[8]

Lignin is present mainly in the middle lammela of the cell walls, where it provides rigidity and structural support to cell walls. The weight percentage of lignin in dried plants is 20-33% but the composition ranges widely between hardwoods and softwoods. The lignin of the middle lammela contains a greater degree of C-C linkages, creating a more condensed and less reactive mesh encircling the outermost layer of the cell wall. Lignin (Figure 2) is a complex cross-linked polymer, produced by radical polymerization of p-hydroxycoumaryl, coniferyl and syringyl aryl-propyl monomers that forms 1,2-diarylpropane-1,3-diol (β-1) and 1-aryl-2-aryloxy-1,3-propaanediol (β-O-4) structures. The aryl rings with one, two or three methoxy groups are often connected to one another through phenolic ether linkages.[8]

The lignin polymer creates a recalcitrant mesh entrapping the carbohydrate rich portions of the cell wall. The essential difference between lignin in hardwoods and softwoods is the number of methoxy groups on the aryl rings of the polymer. Softwoods form from the polymerization of coniferyl alcohol, which are formed from guaiacol and thus contain only one methoxy group per aromatic ring. Hardwood lignin, a polymerization product of both coniferyl and sinapyl alcohol, contains two and three methoxy groups per aromatic ring.[9]

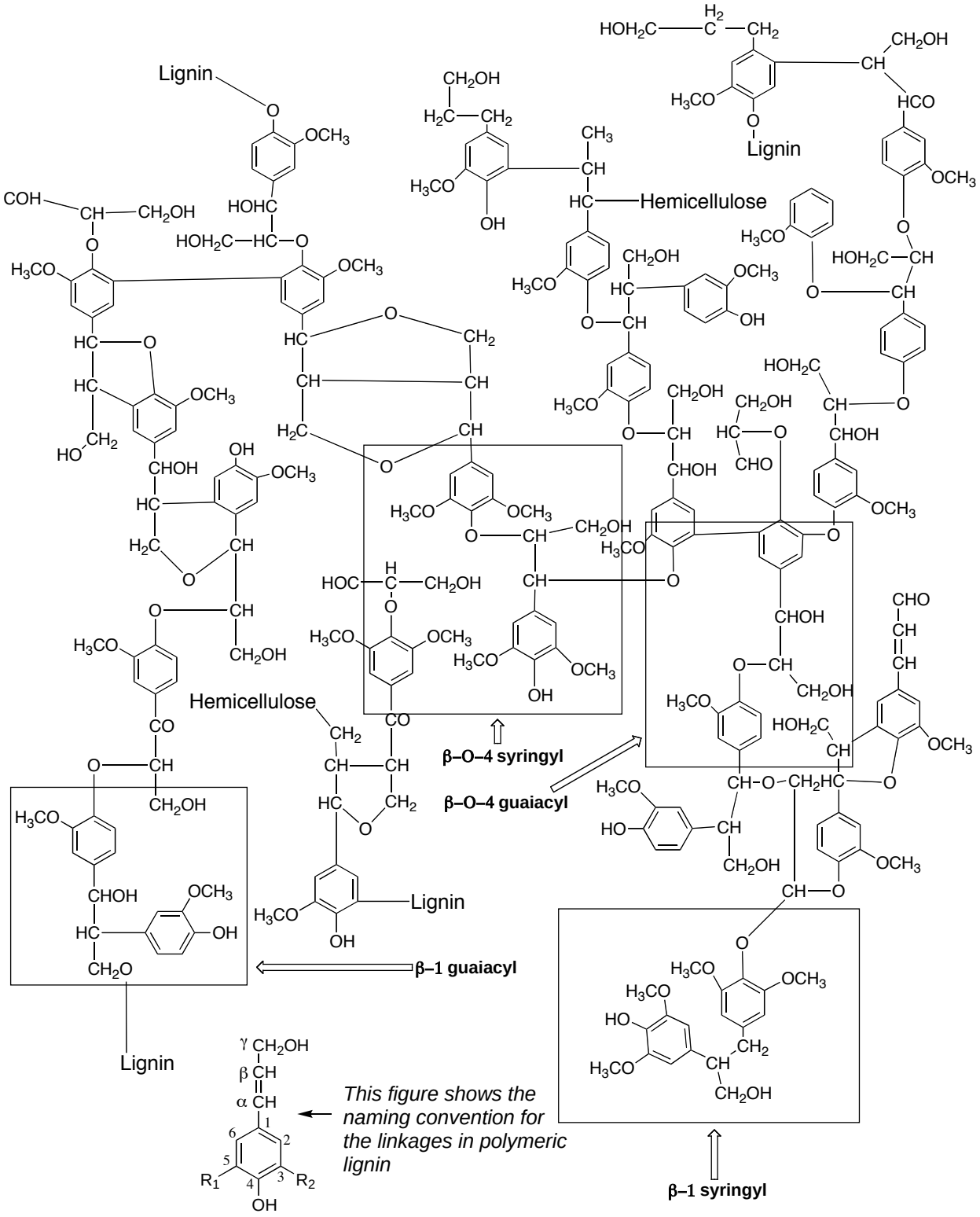

Figure 2. *Representation of the structure of lignin.*

Lignin. The main difficulty in using plant materials as a source of glucose is associated with the fact that plants over a millions of years of evolution have created a protective lignin mesh for the polysaccharide. By natural design, the lignin in plants is recalcitrant to chemical and biological degradation. Thus lignin degradation to obtain cellulose requires the use of high temperatures and extensive milling, harsh chemical conditions, such as extreme pHs and expensive solvents. Unfortunately, this can also result in degradation of the desired plant components, as well as having deleterious effects on the fermentative processes.[10]

Hardwoods and softwoods contain lignins and polysaccharides of different chemical composition. For example, the hemicellulose of softwoods is composed mainly of galactoglucomannan, with arabinoglucoronoxylans as a minor constituent. Hardwood hemicellulose is primarily a glucuronoxylan polymer, with glucomannans as a minor constituent. In addition, softwood lignin is a polymerization product of mainly coniferyl alcohol derived units, forming a guaiacyl type lignin where as hardwood lignins are a co-polymer of coniferyl alcohol and syringyl alcohol derived monomers. The primary difference in these lignins is the number of methoxy functional groups on each aromatic ring. Additionally, hardwood lignin contains fewer free phenol functionalities than softwoods, but more benzyl alcohol groups.[8]

It is interesting that the amount of lignin varies throughout various parts of an individual plant. For example, so called tension wood, specific to hardwoods,

contains an additional cell wall layer, a gelatinous or “G” layer composed entirely of cellulose. The analogous compression wood of softwoods contains less sugars and more lignin.[8-9]

Enzymatic processes that play key roles lignin biosynthesis (Figure 3) are promoted by cinnamate 4-hydroxylase (C4H), 4-coumarate 3-hydroxylase (C3H), O-methyltransferase (OMT), ferulate 5-hydroxylase (F5H), cinnamoyl-CoA reductase (CCR), hydroxycinnamoyl CoA transferase (HCT), and cinnamyl alcohol dehydrogenase (CAD). Alteration of these pathways through up or down regulation has been used to modify lignocellulosic biomass content.[11]

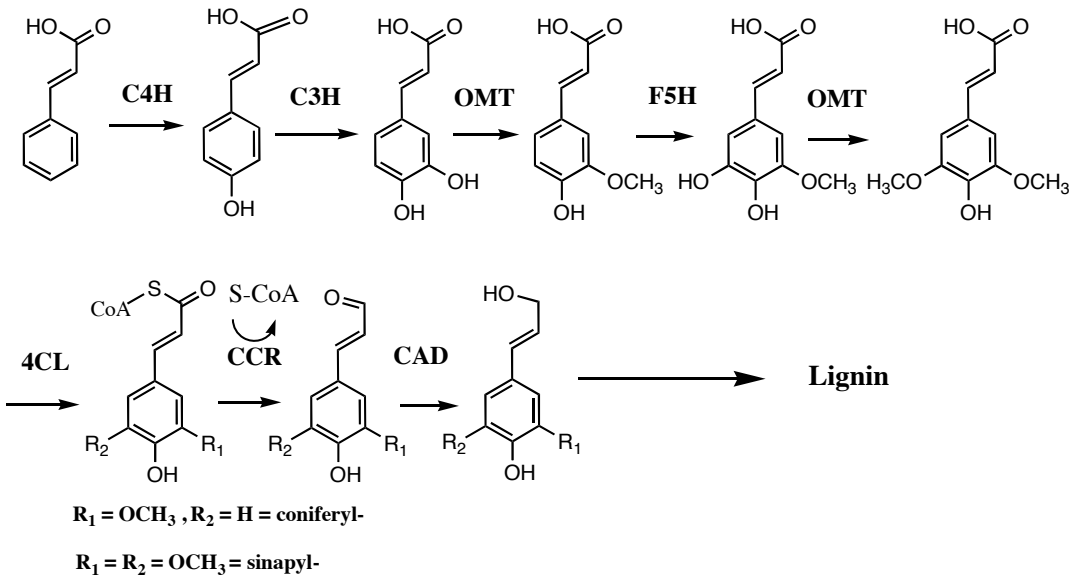

Figure 3. *General Biosynthetic Pathway to Lignin Formation in Wood.*[11]

Hu et al. gained insight into the pathways plants use to accomplish the variation of structural units by studying quaking aspen (*Populus tremuloides*). They found two distinct, 4-coumarate:CoA ligase (4CL) enzymes present in different areas in the plant, which regulated the formation of different

phenylpropanoid structural units. The 4CL genes are known to be necessary for regulating the expression of enzymes responsible for maintaining a steady supply of the substrates needed to synthesize phenylpropanoids, such as lignin and flavonoids, by catalyzing cinnamic acid derivatives to CoA thioesters. The thioesters are then further modified and then incorporated into the lignin polymer. The existence of a compartmentalized functionally diverse enzyme pathway is significant because it sheds light on how common structural units are diverted to produce specialized and diverse cell wall components, such as guaiacyl and syringyl type lignins.[11]

Ralph et al. looked at differing amounts of arylpropane-1,3-diols in normal and mutant CAD deficient pines and identified a radical pathway for their formation (Figure 4). These diols are similar to compounds formed through β-1 model breakdown by lignin peroxidase. CAD is responsible for the reduction of coniferaldehyde to coniferyl alcohol, the final step before incorporation of the monomer into lignin. When CAD is downregulated, coniferaldehyde accumulates and is only inefficiently reduced to coniferyl alcohol. Instead it becomes directly cross-linked with other coniferaldehyde units. Because this process is not as efficient as the CAD mediated process, it is necessary for the plant to utilize alternate pathways of lignin synthesis. This is demonstrated by studies, which show that a monomer found at low levels in normal pines is incorporated in significant amounts in the mutant pine. This finding shows that, while control of the lignin synthesis pathways is possible, alternate existing pathways, although not preferentially used, are present to take their place[12-13].

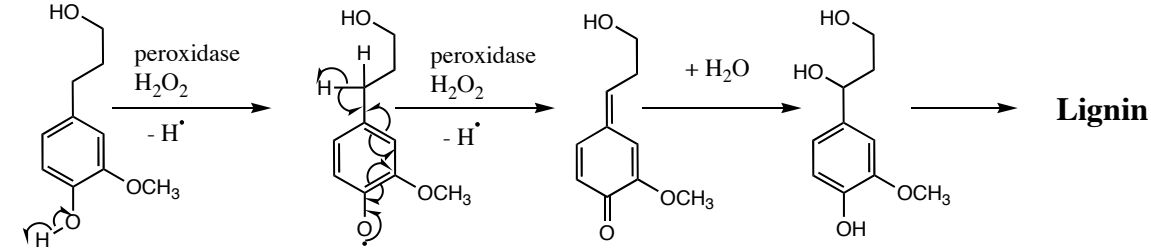

Figure 4. *Radical Mechanism Proposed for Alternate Lignin Synthesis Pathway in CAD Deficient Pines.*[13]

The hope is that the alternate pathways are not primary because, if not, more highly degradable lignin can be genetically engineered into plants. Evidence for this is seen in the increased cell wall degradability of lignin formed with large proportions of coniferaldehyde units. Degradability can be up to 50 % greater in CAD deficient mutants when compared to normal varieties.[14] Other changes in CAD deficient mutants include lower levels of p-coumarate esters, ferulate ethers, and syringyl and guaiacyl contents, and an increase in unusual phenylpropanes and aldehydes. Additionally, less cross-linking with structural polysaccharides in coniferaldehyde lignin is seen.[14] However, Grabber has argued that despite targeted regulation of specific pathways in lignin biosynthesis, compensating changes in other cell wall characteristics often occur. This can create difficulty when attempting to elucidate underlying mechanisms or determine reactivity of certain lignins. For example, mutant plants might respond to reduced lignin content by increasing cross-linking and, as a result, there could

be no noticeable net change in the reactive or nutritive properties of the altered polymer. Due to the complexity of the developing cell wall, this masking effect makes drawing correlations between lignin characteristics such as monomer composition and cell wall degradability more complex and extra care must be taken with respect to interpretation of results and experimental methods when dealing with transgenic modification.[14]

Other studies have shown that the ferulate-5-hydroxylase (F5H) gene regulation can alter lignin composition. F5H expression controls lignin monomer and tissue specificity of syringyl type monomers by catalyzing an irreversible hydroxylation step, diverting ferulic acid from guaiacyl lignin formation toward syringyl type lignin.[15] F5H deficiency results in the formation of only guaiacyl lignin, which, with only one methoxy group, are less amenable to enzymatic degradation.[15] Meyer et al. showed that by attaching a C4H promoter sequence to a chimaeric F5H gene, substantial up-regulation resulted in almost complete syringyl lignin content in some transgenic lines. The cauliflower mosaic virus promoter sequence, a strong non-tissue specific promoter commonly used in plant genetic transformation was initially attached to the F5H gene and tested for upregulation. Levels of F5H were 10 – 60 times higher than the wild type, and tissue specificity was removed, allowing syringyl type monomers to be deposited in vascular tissue as well as supportive tissue. However, there was a limit to the amount of syringyl units accumulated in the transformed lignin, with no more than 35 mole percent observed. Through the use of the C4H promoter sequence, which more specifically targets gene expression to lignifying cells, they were able

to promote F5H expression in the cells responsible for lignin precursor synthesis. This alteration facilitated the F5H pathway to syringyl lignin, resulting in nearly complete syringyl lignin content. Syringyl lignin is rare in nature, and enriched syringyl content lignin is thought to be more amenable to degradation and ruminant digestion.[15]

Chen and Dixon looked at C4H, HCT, C3H, OMT, and F5H down-regulation in transgenic alfalfa by introducing antisense constructs.[16] They report the lowest lignin content in C4H, C3H, and HCT, with lignin content as low as 50 % of wild type plants, and reported F5H having the highest lignin content. This could be an indication that down-regulation at the beginning of the lignin biosynthetic process is most effective. However, strong down-regulation of these genes resulted in a 40 % decrease in biomass produced by the plants. Perhaps most interesting, they found a correlation exists between decreased lignin and increased sugar content, with some transgenic plants showing a 2-fold increase of sugar content over wild type plants. Additionally, the decreased lignin content increased the sugar yield upon treatment with enzymatic and traditional acid pretreatment methods. Combining acid pretreatment and enzymatic hydrolysis increased saccharification efficiency by as much as 79 %, with up to 90% of the sugar released being glucose. This clearly shows the enhanced ability of the enzyme to penetrate the cell wall polysaccharides. These transgenic methods of up-down-regulation are exciting, especially when one considers that the pathways of lignin biosynthesis are conserved across the plant kingdom.[16-17] This means the development of strategies in one transgenic species could be applied in a more

general fashion. Since the most likely future sources of biomass will need to be hardy and fast growing non-deciduous species, such as grasses and small shrub-like species, containing large amounts of non-methoxylated p-hydroxycoumaryl lignin structure, the work of Chen and Dixon is an important step in the potential bio-alteration of these least reactive lignin monomers.

Enzymatic Lignin Degradation. Several species of insect are known to degrade wood and use it as a food source. Termites exist in a symbiotic relationship with microbe(s) capable of depolymerizing lignin and cellulose. Additionally, some beetle species use a fungal symbiote of a soft-rot variety.[18] Many species of microorganisms are of interest in the context of biomass conversion. Many of these organisms use free cellulase enzymes, in contrast to large multi-enzyme cellusomes, to degrade cellulose. Some have the capability of using other sugars present in hemicellulose, such as xylose and mannose.[19] Bioengineering these organisms to degrade lignin or improve fuel yield by conversion of these other sugars would benefit the use of biomass as an energy source.

To date, the only known process by which biomass, and particularly wood, can be completely degraded is through pathways employed by various species of *Basidomycete* fungi known as “white rot” fungi. These fungi release complex mixtures of enzymes and cofactors, which act to degrade wood to a fine white powdery substance. Under certain conditions, the fungi express enzymes and cofactors that act in conjunction to depolymerize lignin, exposing cellulose, which is subsequently utilized by the organism as a food source.[20-22] These enzymes

are expressed under limited nitrogen conditions and have maximal activity at low pH, both conditions which are present in intact wood.[7-9]

Much interest has been given to the use of these fungi in paper pulp processing, and most of the early work involving fungal peroxidases was aimed at facilitating the paper making process. Delignifying wood pulp to a certain extent (but not completely) aids the achievement of desirable characteristics in finished paper. Perhaps the most exciting potential of white rot fungi are there use as biomass degraders. The white rot fungi employ a cadre of enzymes, which act in a synergistic fashion to degrade the recalcitrant components present in wood cell walls and specifically lignin. The substances excreted by the fungi include cofactors, such as hydrogen peroxide and mediators such as veratryl alcohol. Furthermore, some of the substrates of these extracellular excretes are derived from the breakdown of wood itself, allowing continuation of the cycle.[20] The enzymes excreted by white rot fungi that are of particular interest in terms of biomass conversion to ethanol are members of the peroxidase family. Particularly, lignin peroxidase (LP) is of interest due to its ability to oxidatively degrade a wide variety of substrates.[23-24]

Considerable attention has been given to the fungal peroxidases over the past 30 years and reports of the use of “mushroom peroxidases” to probe the molecular structure of lignin date back to the 1950’s.[9] The isolation of a lignin degrading enzyme from the extracellular medium of laboratory grown cultures of the white rot fungi *Phanerochaete chrysosporium* and subsequent isolation of

another peroxidase dependent on manganese as a cofactor, stimulated a great deal of ensuing investigations.[25]

The results of early work of Kirk, Tien, and others described characteristics of the lignin degrading enzymes later known as LP and manganese peroxidase that are found in a number of white rot fungi. The later discovery of the wood degrading oxidase enzyme, laccase, and another peroxidase, the so called versatile peroxidase, which had the capacity to carry out the same degradation processes as both lignin peroxidase and manganese peroxidase, was also intriguing.[26] Despite receiving intense attention, the actual mechanism of lignin breakdown in the natural environment is still not resolved. Furthermore, questions remain as to whether the organism uses the oxidase enzymes to form mediator oxidants that diffuse into the areas of the plant in which the enzyme cannot cross or whether there is a direct interaction of the enzymes with lignin through long-range electron transfer mechanisms. Analysis of the structure of the enzyme shows that no direct binding interaction between the enzymes and lignin can take place.[27-28] Lignin peroxidase catalyzed reactions proceed by a ping-pong mechanism, which consumes two equivalents of substrate following the initial activation step. The mechanism proceeds through cation radical intermediates, and the substrate cation radicals produced follow various pathways depending on the nature of the substrate.[21, 79]

LP is a heme containing enzyme that exists in the Fe(III) oxidation state. There are also two histidine residues near the active site, an upper (proximal) and a lower (distal) one, with the distal histidine assisting in the formation of the

peroxide binding pocket and the proximal assisting in the formation of the substrate binding pocket.[28] In the mechanistic pathway for enzyme catalyzed oxidation reactions of LP substrates, the activator hydrogen peroxide first oxidizes the iron to a Fe(IV) state while also removing an electron from the porphyrin ring to leave a doubly oxidized enzyme form (so called Compound I). A substrate molecule then donates an electron to the heme cation of the doubly oxidized form of LP to produce a substrate cation radical and the singly oxidized form of the enzyme (so called Compound II). In addition, a second substrate molecule donates an electron to reduce the Fe(IV) form of the enzyme to produce the original Fe(III) form.[29-31, 24]

The general chemical pathway for LP promoted oxidation is illustrated by using veratryl alcohol (VA) as the substrate (Figure 5). The pathway begins with the initial

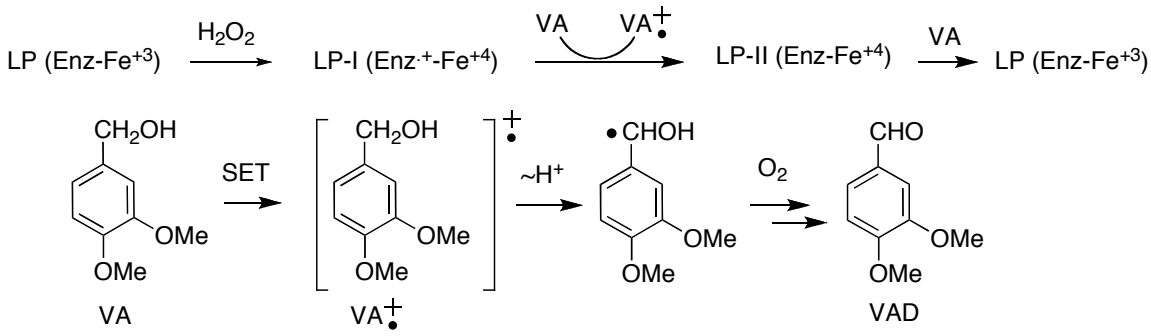

Figure 5. *Mechanism for Lignin Peroxidase Catalyzed Oxidation of Veratryl Alcohol.*

activation step, in which H_2O_2 reacts with the enzyme to generate doubly oxidized LP. VA is then is oxidized by a one electron transfer event, forming the substrate radical cation. A second substrate molecule is oxidized to form a cation radical and the enzyme is reduced to produce its resting Fe(III) neutral state. A third state of LP has been identified (so called Compound III). This state is formed when the enzyme is inactivated by excess hydrogen peroxide. Finally, the cation radical of VA undergoes loss of a proton to give a radical that reacts with molecular oxygen to form veratryl aldehyde (VAD).[30, 34]

Lignin model compounds have been used to gain information about the nature of LP promoted delignification. These efforts show that LP catalyzes a reaction pathway in which C-C bond cleavage takes place. The pathway, depicted for oxidative cleavage of a β-1 model compound in Figure 6, begins electron transfer of the substrate to the doubly oxidixed form of LP to produce a cation radical gives either a diol or hydroxy ketone. A similar mechanism has been proposed for oxidative cleavage of β-O-4 model compounds (Figure 7).[1,30,35]

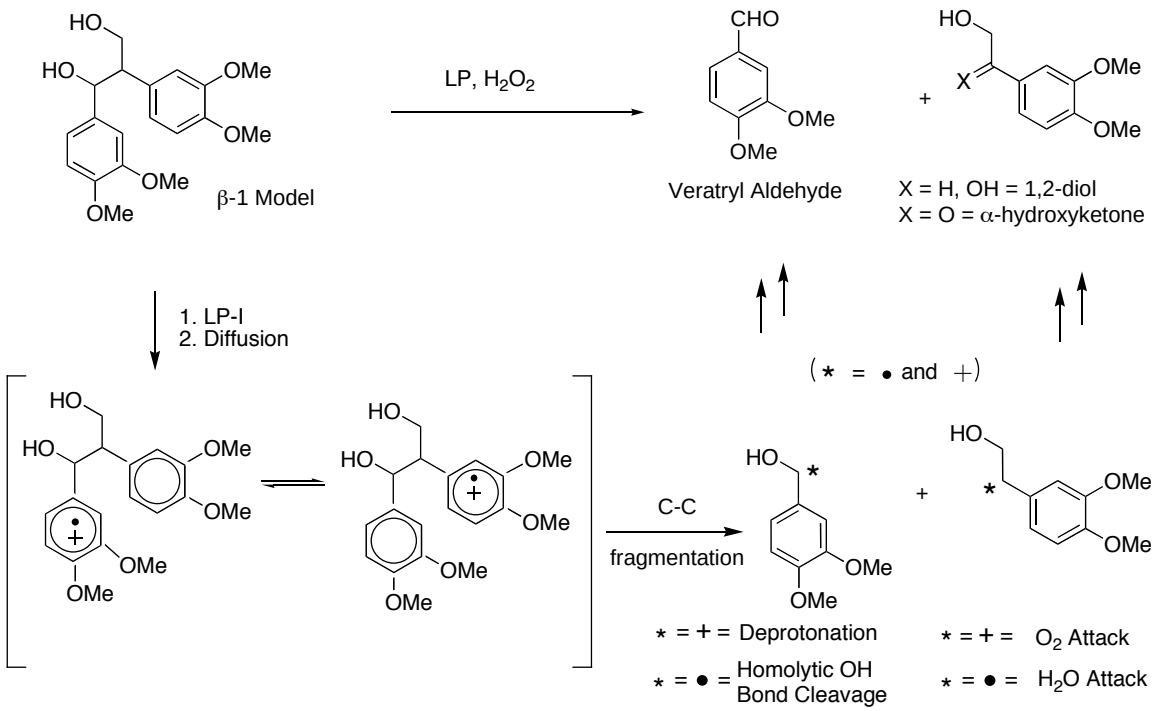

Figure 6. *Proposed Mechanism of LiP Catalyzed β-1 Oxidation.*

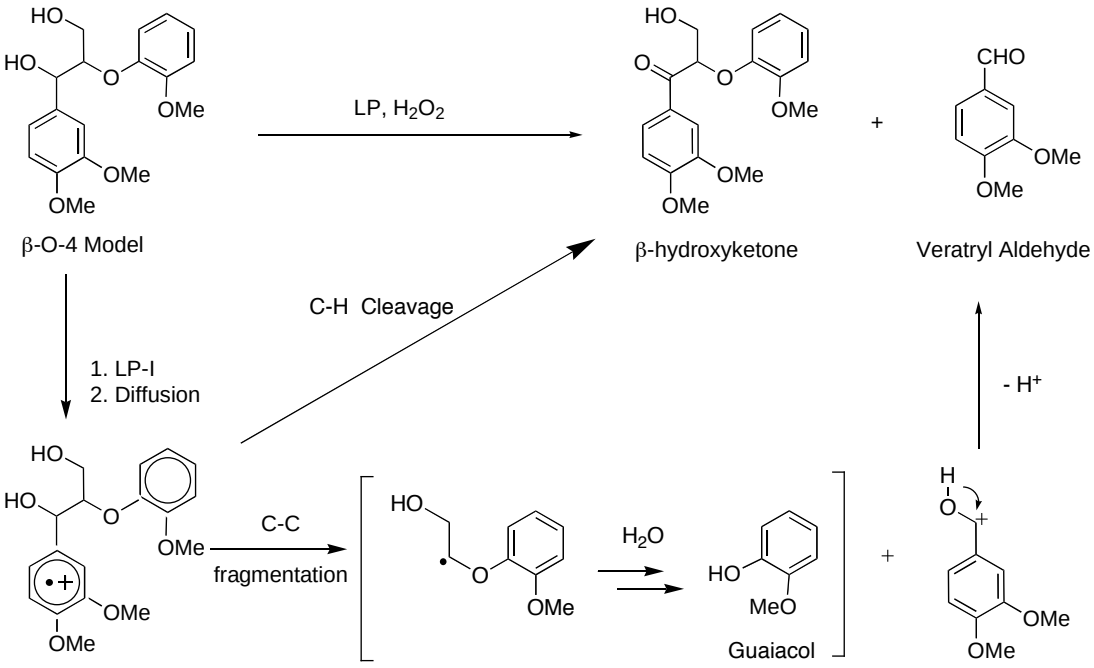

Figure 7. *Proposed Mechanism of LiP Catalyzed β-O-4 Oxidation.*

Purpose of the Investigation

The primary long range issue we set out to address in this investigation concerns the mechanism of C-C bond cleavage of lignin model compounds promoted by LP and other oxidants and the effects of structure (β-1 vs. β-O-4), substituents (one, two or three methoxy groups) and stereochemistry (erythro vs. threo) on the rate of C-C bond cleavage.

In order to probe these issues, we have designed a study to probe several issues regarding oxidative cleavage reactions of lignin model compounds. In our initial effort, the results of which are presented below, diastereomeric dimeric lignin β-1 (**1**) and β-O-4 (**2**) model compounds (Figure 8) were employed to elucidate several important features of the lignin oxidative cleavage process. Cation radicals of these substances, which are models of the major types of structural units found in the lignin backbone, have been generated by using well-understood SET-sensitized photochemical and Ce(IV) promoted oxidative processes and the nature and kinetics of their C-C bond cleavage reactions were determined. In addition, lignin peroxidase catalyzed reactions of the model compounds were explored in order to determine product distributions and kinetic parameters. My part of this effort focused on the LP and CAN promoted reactions. My work on the LP catalyzed oxidative cleavage reactions of the lignin model compounds concentrate on both the identification of reaction products and the kinetic analyses of the reaction. In addition, I contributed to studies of Ce(IV) promoted reactions of the model compound by carrying out kinetic analyses. The

results of my efforts along with those of Dr. Daewon Cho on Ce(IV) and photochemical reactions of the model compounds are presented below.

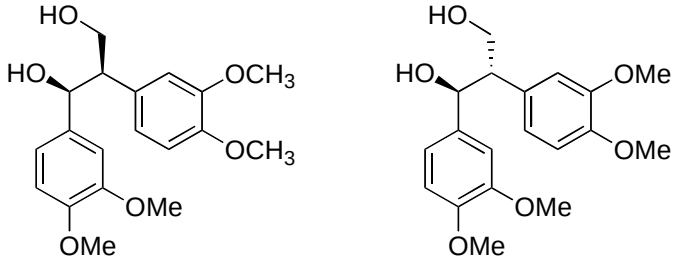

1-Threo **1-Erythro**

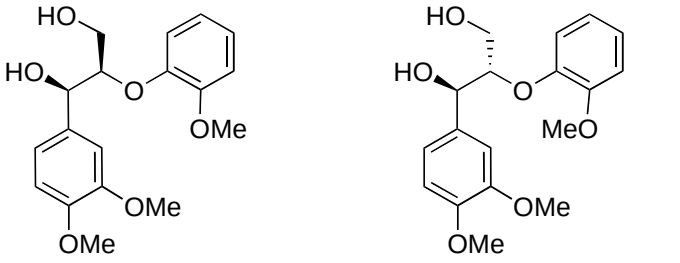

2-Threo **2-Erythro**

Figure 8. *Structures of the Lignin Model Compounds.*

Results

SET-Photochemical Reactions of the Lignin Model Compounds. In order to determine the nature of the pathways followed in reactions of cation radical intermediates, the diastereomeric β-O-4 and β-1 lignin model compounds were subjected to SET-promoted photochemical reactions using 9,10-dicyanoanthracene (DCA) as the excited state electron acceptor. DCA is ideal in this regard since it absorbs light at wavelengths (> 350 nm) that are longer than do **1** and **2** (λ_{max} *ca.* 280 nm), it has a large singlet excited state reduction potential (*ca.* +2.8 V) and a modest singlet lifetime (*ca.* 15 ns), and finally the anion radical formed from DCA by SET is reasonably stable. Irradiation (λ > 330

nm) of 5% aqueous MeCN solutions containing DCA (0.27 mM) and the erythro and threo isomers of **2** (2.1 mM) leads to formation of veratrylaldehyde (VAD), guaiacol **3** and the keto-alcohol **4** (Scheme 3) in the yields given in Table 1.

Scheme 1.

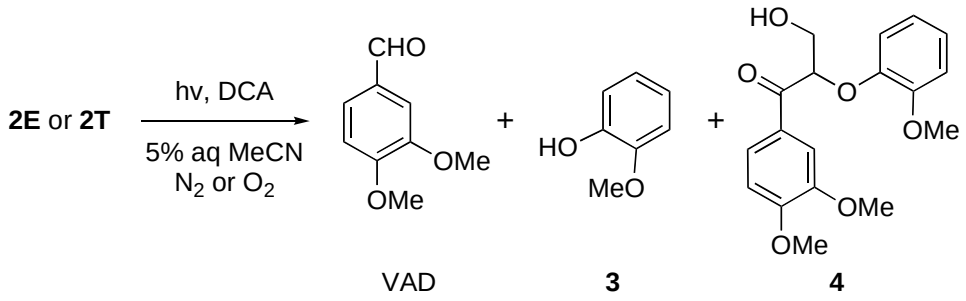

As can be seen by viewing the data given in Table 1, the extent of conversion of the substrates for fixed time irradiations is significantly enhanced in DCA-promoted photoreactions occurring on oxygen saturated solutions of the diastereomers of **2**. In addition, reactions of **2E** and **2T** in the presence of O_2 take place with similar chemical efficiencies but produce different ratios of VAD and keto-alcohol **4** (*i.e.*, VAD:**4** from **2E** = 10:1 and from **2T** = 3:1).

DCA-induced photoreactions of the β-1 model compounds **1T** and **1E** take place more efficiently (as determined by irradiation time *vs.* conversion) than those of the β-O-4 analogs under identical conditions. These photoreactions generate VAD, diol **5** and keto-alcohols **6** and **7** (Scheme 4, Table 1). Importantly, keto-alcohol **6** along with VAD is generated when diol **5** is subjected to the DCA-promoted photochemical reaction conditions.

As with the β-O-4 model compounds, DCA-induced photoreactions of **1T** and **1E** yield VAD as the major product and substrate conversions for fixed time

irradiations are enhanced when O_2 saturated solutions of these substrates are irradiated (Table 1).

The photoproducts produced in photoreactions of the isomers of **1** and **2** in most cases (VAD, **3**-**4, 5-6**) are known compounds. An authentic sample of the previously reported[80] keto-alcohol **7** was prepared for spectroscopic and chromatographic comparison purposes by using a sequence involving TBDPS primary alcohol protection, secondary alcohol oxidation and alcohol deprotection In order to evaluate the reactivities of cation radicals derived by SET-oxidation, relative quantum yields of the DCA-promoted photoreactions of the isomers of **1** and 2 were determined. Relative quantum efficiencies (ϕ_{rel}) were measured by using the standard simultaneous irradiation technique, in which equivalent concentrations of DCA and substrates are irradiated for equivalent time periods that bring about low substrate conversions (*ca.* 10%) (Supporting Information). The data obtained from these experiments is given in Table 2.

Scheme 2.

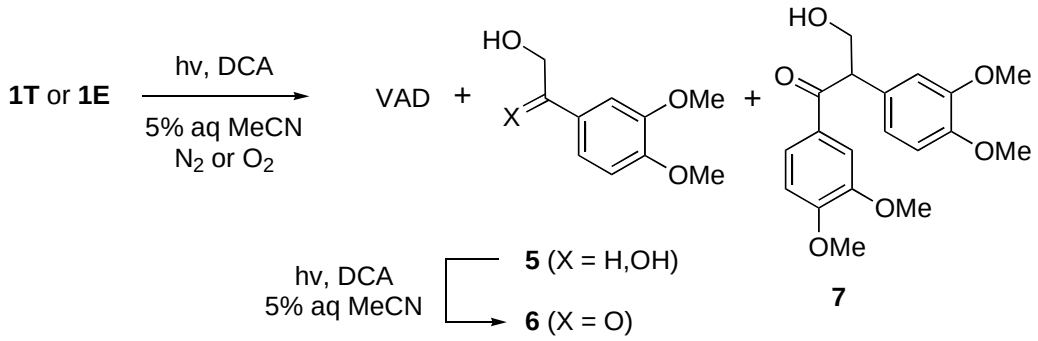

Table 1. Products and Yields of DCA-Promoted Photoreactions of the Lignin Model Compounds.

Substrate	Conditions[a]	Percent Conversion[b]	Percent Yields[c] (Based on Recovered Starting Materials)					
			VAD	**5**	**6**	**3**	**4**	7
1T	N_2 Satd	52	44 (85)	8 (15)	14 (27)	--	--	4 (8)
1T	O_2 Satd	100	95	trace	28	--	--	--
1E	N_2 Satd	46	40 (87)	4 (9)	7 (15)	--	--	trace
1E	O_2 Satd	100	96	trace	40	--	--	--
2E	N_2 Satd	5	4 (80)	--	--	trace	--	--
2E	O_2 Satd	88	45 (51)	--	--	3	4 (5)	--
2T	N_2 Satd	5	4 (80)	--	--	trace	--	--
2T	O_2 Satd	90	55 (61)	--	--	5 (6)	20 (22)	--

[a] Irradiation, using uranium glass filtered light, of 5% aq MeCN solutions of DCA (0.27 mM) and substrate (2.1 mM) saturated with either N_2 or O_2 for 7 h at 25°C.
[b] Based on recovered starting substrates, determined by HPLC analysis.
[c] Yields, determined by using HPLC.

Table 2. Relative Quantum Yields of Photoreactions, Oxidation Potentials and Rates of DCA-Fluorescence Quenching of the Lignin Model Compounds,.

Substrate	ϕ_{rel}[a]	$(E^{S_o}_{1/2}$ (+) (V)	$k_q \times 10^{-10}$ ($M^{-1}S^{-1}$)
1T	6.5	1.18	1.24
1E	7.7	1.22	1.16
2E	1.9	1.22	1.16
2T	1.0	1.19	0.99

[a] Relative quantum yields for formation of VAD.

To insure that the relative quantum yields reflect the reactivities of the cation radicals produced by SET to the singlet excited state of DCA (DCA^{S1}) and not the rates of SET to DCA, fluorescence quenching measurements were made. The results displayed in Table 2 show that, in each case, the β-1 and β-O-4 model compounds quench the fluorescence of DCA at near equal diffusion controlled rates. This is an expected result based on the fact that the measured oxidation potentials ($E^{S_o}_{1/2}$ (+)) of the isomers of **1** and **2** (Table 2) all fall well below the reduction potential of DCA^{S1} (+2.8 V).

Ceric Ammonium Nitrate (CAN) Promoted Reactions of the Lignin Model Compounds. SET oxidation reactions of the isomers of **1** and **2**, promoted by the one electron oxidant CAN, also take place predominantly by way of C-C bond cleavage to yield VAD as the major product. For example, reactions of the erythro and threo isomers of the β-O-4 model compound, **2E** and **2T**, with 2 equivalents of CAN in MeCN at 25°C give rise to VAD, keto-alcohol **4**, and a nitro-substituted keto-alcohol **8** of unassigned regiochemistry (Scheme 5, Table 3). The latter substance was shown to arise by secondary CAN oxidation of **4**.

Scheme 3.

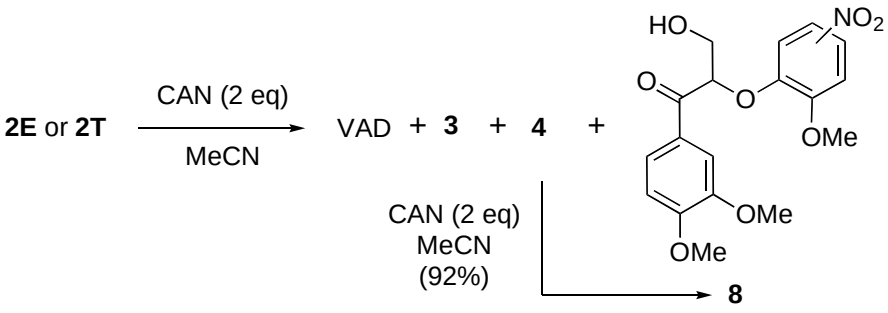

Table 3. Products and Yields of CAN Promoted Reactions of the Lignin Model Compounds.

Substrate	Percent Conversion[a]	Percent Yields[b] VAD	**6**	**3**	**4**	**7**	**8**
1T	100	95	25	--	--	trace	--
1E	100	95	46	--	--	trace	--
2E	90	88	--	trace	7	--	4
2T	96	31	--	trace	32	--	33

[a)] Reaction of CAN (1.0 mM) and lignin model compound (0.5 mM) in MeCN at 25°C for 15 h.
[b)] Yields determined by using HPLC analysis.

Interestingly, CAN oxidations of the erythro and threo isomers of **2** give rise to dramatically different ratios of VAD and keto-alcohol **4**. Specifically, while **2E** yields VAD nearly exclusively, near equal amounts of VAD and **4** are produced by reaction of **2T** under equivalent CAN oxidation conditions. This trend is not observed in CAN oxidations of the β-1 models, **1T** and **1E**, where VAD is the predominant product formed along with keto-alcohols **6** and **7** (Scheme 6, Table 3).

Scheme 4.

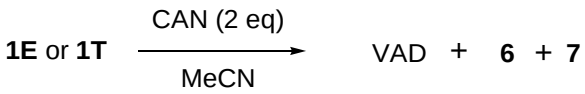

CAN induced oxidation reactions of arenes are known to take place by pathways involving initial SET to Ce (IV) followed by rate limiting reactions of the formed cation radical intermediates (*eg.*, proton transfer, C-C bond cleavage).

As a result, the rates of CAN oxidations of the lignin model compounds should reflect the reactivity of the initially formed cation radicals. When framed in the context of VAD production, the rates of these processes will be a measure of the rate of cation radical C-C bond cleavage.

As can be seen by viewing the plots shown in Figure 5, absorbances of CAN (2.5×10^{-4} M initially) at 390 nm in MeCN solutions containing 1.25×10^{-4} M

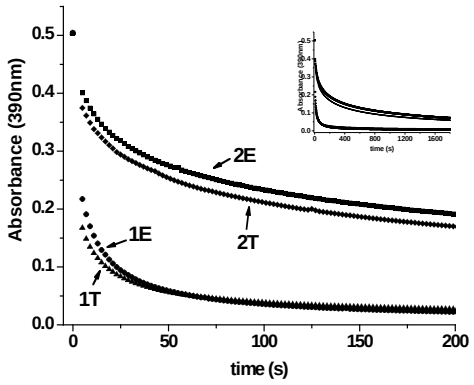

Figure 9. *Plots of the absorbances at 390 nm of CAN solutions (initially 2.5 x 10^{-4} M) in MeCN at 25°C containing 1.25 x 10^{-4} M* ***1T****,* ***1E****,* ***2E****, and* ***2T*** *as a function of time.*

of the lignin model compounds decrease as a function of time. In each case, the absorbance reaches a constant value after 2 equivalents of CAN are consumed. A qualitative interpretation of these plots show that the rates of the CAN oxidation reactions are dependent on the nature (β-1 *vs.* β-O-4) and stereochemistry (threo *vs.* erythro) of the substrates.

Accurate rate constants for the CAN oxidation reactions of the stereoisomers of **1** and **2** were determined by measuring the initial rates of disappearance of CAN (0.1-2.5 s) by using the stopped flow kinetic technique. Kinetic analyses were carried out under two different conditions including (1) 3.5×10^{-4} M lignin model compounds and varying concentrations (1.5×10^{-4} to 3.6×10^{-4} M) of CAN (Figure 10A), and (2) 3.0×10^{-4} M CAN and varying concentrations (7.5×10^{-5} to 3.75×10^{-6} M) of the lignin models (Figure 10B). The slopes of these plots (at <10% conversion of substrate) give bimolecular rate constants for the oxidation reactions and, consequently, the rates of reactions of the cation radicals arising from the diastereomers of **1** and **2** (Table 4).

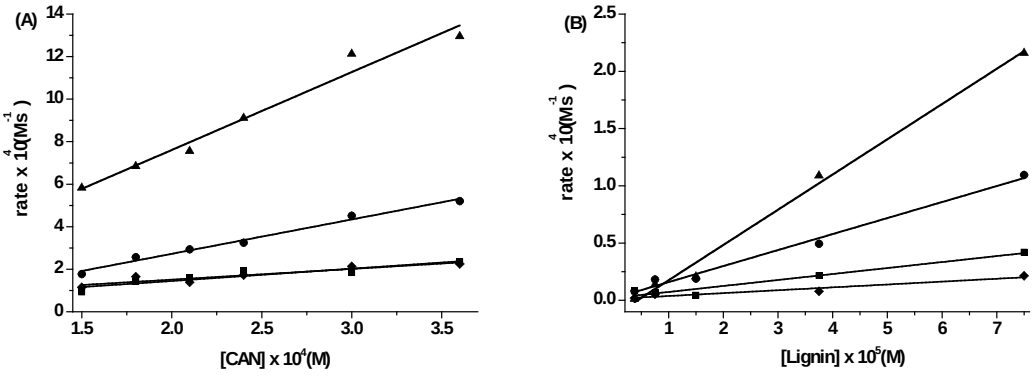

Figure 10. *Plots of the rates of CAN oxidations of **1T** (▲), **1E** (●), **2E** (■), and **2T** (♦) as (A) functions of the concentration of CAN at fixed concentrations of **1T**, **1E**, 2**E**, and 2**T** (3.75 x 10^{-4} M), and (B) functions of the concentrations of **1T**, **1E**, **2E**, and **2T** at fixed concentrations of CAN (3.0 x 10^{-4} M). The reactions were carried out by using MeCN solutions of the reactants at 25°C for time periods of 0.1-0.25 s.*

Lignin Peroxidase Catalyzed Reactions of the Lignin Model Compounds. Lignin peroxidase (LP) promoted oxidation reactions of the diastereomeric β-1 and β-O-4 lignin models were explored in order to determine the nature and yields of the products formed. All of these processes were carried out in tartrate buffered solutions (pH 3.4) containing the substrates (200 μM), LP (0.36 μM) and hydrogen peroxide (100 μM) for varying time periods. HPLC analysis of each reaction mixture showed that the diastereomeric β-1 models **1T** and **1E** undergo LP catalyzed reactions that generate VAD, diol **5** and keto-alcohol **6** as major products in the yields given in Table 5. In addition, VAD and keto-alcohol **4** are produced as major products along with minor amounts of guaiacol **3** in LP promoted oxidations of the β-O-4 erythro and threo isomers **2E** and **2T**.

Table 4. Rate Constants for CAN Oxidations of the β-O-4 and β-1 Lignin Model Compounds.

Substrate	$k \times 10^{-2}$ $(M^{-1}s^{-1})^a$	$k \times 10^{-2}$ $(M^{-1}s^{-1})^b$
1T	98±8	103±5
1E	43±2	47±3
2E	15±3	17±2
2T	14±3	8±2

[a)] Determined by varying the concentration of CAN at fixed concentrations of the lignin model compounds.
[b)] Determined by varying the concentration of the lignin model compounds at fixed CAN concentrations.

Table 5. Products and Yields of Lignin Peroxidase Catalyzed Reactions of the Lignin Model Compounds.

Substrate	Percent Conversion[a]	Percent Yields[b] (Based on Recovered Starting Matls.)				
		VAD	**5**	**6**	**3**	**4**
1T	73	52 (71)	trace	14 (19)	--	--
1E	77	45 (58)	--	15 (19)	--	--
2E	35	30 (86)	--	--	trace	4(11)
2T	66	31 (47)	--	--	trace	29(44)

a) Reactions carried out using 200 μM substrate, 0.36 μM LP, 100 μM H_2O_2 in tartrate buffered solutions (pH 3.4).
b) Yields, determined by using HPLC.

As reflected in the percent conversions in the fixed time reactions, the rates of LP catalyzed oxidations of the model compounds depend on both type and stereochemistry. A semi-quantitative analysis of the rates of these processes was conducted by following the increase in absorbance at 310 nm, corresponding to formation of VAD and keto-alcohols **4** and **6**. For each solution containing fixed substrate (200 μM), LP (0.36 μM) and H_2O_2 (100 μM) concentrations. As can be seen by viewing the plots obtained in this manner (Figure 11), the β-1 models **1T** and **1E** undergo LP-induced cleavage to produce VAD at higher rates than the β-O-4 analogs. In addition, in the β-1 series the threo isomer **1T** is most reactive, the erythro isomer **1E** while in the β-O-4 series the two diastereomers are about equally reactive.

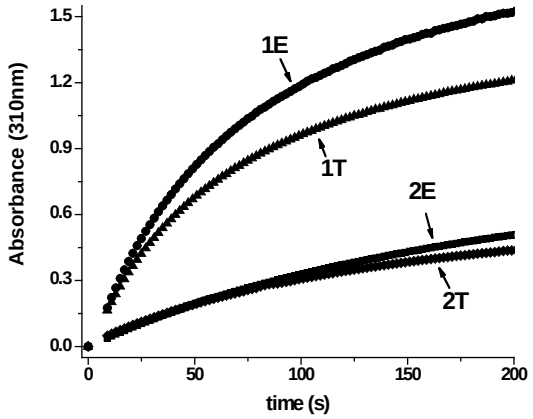

Figure 11. *Absorbance (310 nm) as a function of time plots for LP (0.36 μM) catalyzed oxidative cleavage reactions of the lignin model compounds* ***1T****,* ***1E****,* ***2E*** *and* ***2T*** *(200 μM) in tartrate buffered solutions containing H_2O_2 (100 μM).*

As a consequence of the instability of LP in the presence of H_2O_2, a substance required for production of the activated form of the enzyme, the plots shown in Figure 11 reach maximum values at *ca.* 200 s that do not reflect complete consumption of the starting substrates. This phenomenon prevents an accurate assessment of the kinetic constants for these processes. To solve this problem, the stopped-flow method was employed to determine the rates of LP catalyzed reactions of the diastereomeric lignin models in time frames where LP degradation by H_2O_2 is not problematic. In a stopped flow apparatus, solutions of LP (1.8 μM) in tartrate buffer (pH 3.4) containing H_2O_2 (50 μM) were mixed with solutions containing from 50 to 2500 μM of **1T, 1E, 2E** and **2T**. The absorbance increases at 310 nm corresponding to the formation of VAD and keto-alcohols **6**

and **4**, were measured over a 0.1-1 s time period. The slopes of these plots arising from saturate concentrations in the range of 50-2500μM give rates which are used to construct velocity (v) versus concentration ([S]) (see Figure 20) and 1/v versus 1/[S] (Lineweaver-Burk) plots from which the k_{cat} and K_M values listed in Table 6 are derived (see Figure 21). It should be noted that the v versus [S] plots show saturation kinetic behavior that is typical for enzymatic reactions that involve initial equilibrium binding of the substrate to the enzyme.

Table 6. Steady State Kinetic Constants for Lignin Peroxidase Catalyzed Reactions of the β-O-4 and β-1 Lignin Model Compounds.

Substrate	k_{cat} (s^{-1})	K_M (μM)	k_{cat} / K_M x 10^3 ($\mu M^{-1} s^{-1}$)
1T	3.85	46.6	83
1E	9.23	254	36
2E	0.50	155	3
2T	1.14	134	9

Discussion

The overall aim of our investigations in the area of lignin chemistry is to gain fundamental information about the factors that govern the oxidative carbon-carbon bond cleavage reactivity of various 1,2-diaryl- and 1-aryl-2-aryloxy-propanoid units in this structurally and stereochemically complex natural polymer.

The hope is that knowledge gained in these efforts will aid in the design of methods that can be used to degrade lignin in a mild, efficient and cost effective manner as part of processes that transform plant materials into ethanol. In the context of ethanol production from plant materials, mild and efficient methods are needed to deconstruct lignin and, thereby, enable access to cellulose by enzymes that promote its hydrolytic transformation to glucose. Among the most promising approaches for this purpose involves the use of enzymes derived from wood rotting fungi, like *phanerochaete chrysosporium*, which are known to degrade lignin in plants.[29, 36-38] The most studied of these enzymes is lignin peroxidase (LP), which contains an iron-heme redox active center.[23, 25 ,28, 37 ,39, 40-42] It has been proposed that LP promoted delignification results from oxidative C1-C2 bond cleavage of aryl propanoid moieties by way of a mechanism that is initiated by single electron transfer (SET) from aryl donor sites to the Heme^{+1} - Fe^{+4} form of the enzyme. Key events in the degradation pathway are C-C bond cleavage reactions of aryl ring centered lignin cation radicals. This processes, which mimic reactions of 1,2-diarylethanes and 1-aryl-2-ethyl ethers (Scheme 5),[43-55] result in the generation of cation radical pairs in which odd electron and positive charge distributions are governed by thermodynamics. As has been pointed out previously and experimentally demonstrated in thorough studies by Arnold and his coworkers,[43-50] the C-C bond cleavage reactions of cation radicals of these types of substrates can be viewed as being either heterolytic or homolytic in nature and, in either case, they yield the most stable radical and cation intermediates. Perhaps more significant are observations made by

Arnold[43-50] and Maslak[51-55] which show that the rates of C-C bond cleavage of 1,2-diarylethane and 1-aryl-2-ethyl ether cation radicals parallel cation radical C-C bond dissociation energies. This important concept will be fully discussed below following a discussion of reaction mechanisms and observations leading to the assignments of C-C bond cleavage rates of the diastereomeric β-1 and β-O-4 lignin model compounds.

Scheme 5.

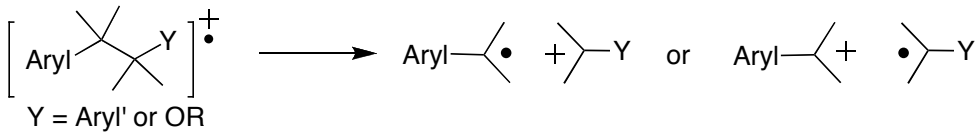

Reaction Mechanisms. In this investigation, three methods were used to generate cation radicals of the diastereomeric β-1 and β-O-4 lignin model compounds. The first of these involves the use of a SET-photochemical route in which the UV-irradiation generated singlet excited state of DCA (DCA^{S_1}) ($E_{½}$ (-) = +2.8 V) serves as the oxidant. As demonstrated by the results of DCA fluorescence quenching experiments, the lignin model compounds quench DCA^{S_1} at near equal, diffusion controlled rates (*ca* 1 x 10^{10} M^{-1} s^{-1}). Owing to the low oxidation potentials of the model compounds ($E_{½}$ (+) *ca* 1.2 V, Table 2) and the fact that the energies of their singlet excited states are much higher than that of DCA, the quenching process takes place by thermodynamically driven (ΔG^{0}_{SET} = ca -1.6 eV) SET.[56]

As in the case of reactions initiated by other oxidants, the cation radicals, produced by photoinduced SET of the β-1 and β-O-4 model compounds, undergo

predominant C1-C2 bond cleavage to form radical cation pairs. Based on a qualitative evaluation of oxidation potentials,[57] cation radicals arising from the β-1 models **1T** and **1E** have charged radical centers that are nearly equally distributed in both the 1- and 2-aryl rings (Scheme 6). A consideration of approximate oxidation potentials of the two

Scheme 6.

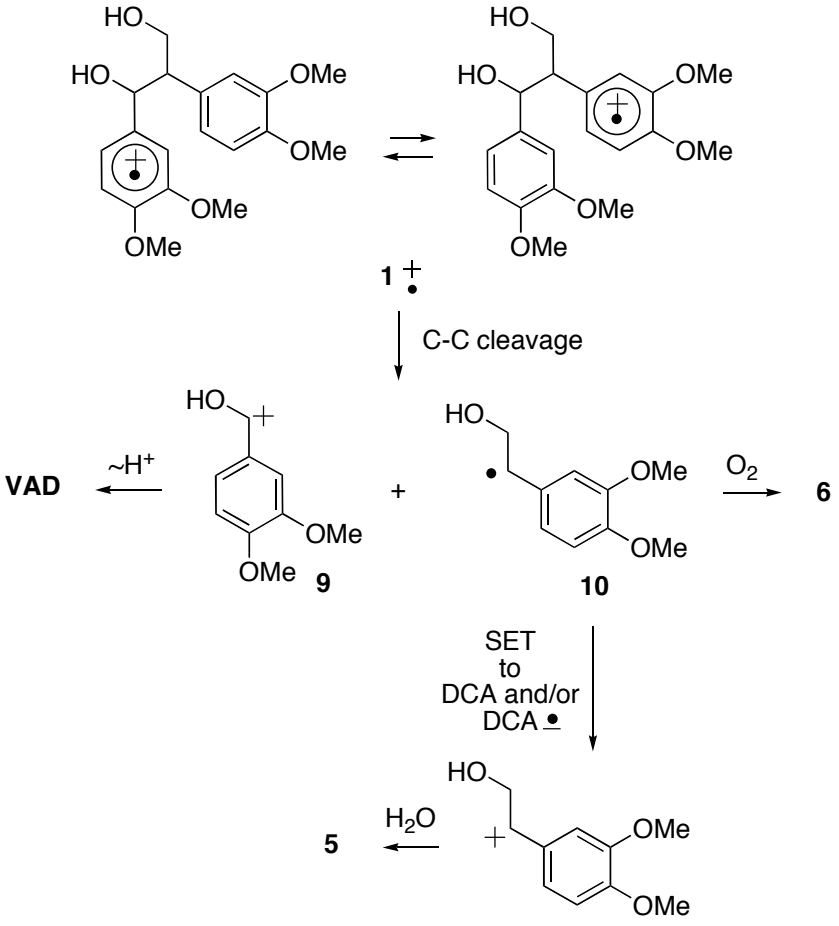

radicals that could be produced suggests that C-C bond cleavage of these transients will produce pairs in which the positive charge is located on the α-hydroxylbenzyl fragment **9** and the radical center is located on the α–hydroxyethylbenzyl fragment **10** (Scheme 6). Data which support this

proposal come from the work of Griller and Wayner,[58-60] which shows that oxidation potentials of oxy-substituted radicals are much lower than those of alkyl-substituted counterparts. For example, the α-methoxy-*p*-methoxybenzyl radical has an oxidation potential of -0.51 V whereas the α,α-dimethylbenzyl radical has an oxidation potential of -0.14 V.[59-60] Loss of a proton from **9** gives rise to veratrylaldehyde (VAD), the major product formed in these reactions. The behavior of the radical fragment **10** is different than that observed for related benzylic radicals produced in 1,4-dicyanobenzene (DCB) photosensitized reactions of 1,2-diphenylethane derivatives. In earlier studies, Arnold and his coworkers[47-49] observed that DCB promoted cleavage of 1,1,2,2-tetraphenylethane in 3:1 MeCN-MeOH leads to production of diphenylmethylether and diphenylmethane. The route formation of the latter substance involves reduction of the intermediate diphenylmethyl radical by the anion radical of DCB. Protonation of the resulting anion then forms diphenylmethane (Scheme 7).

Scheme 7.

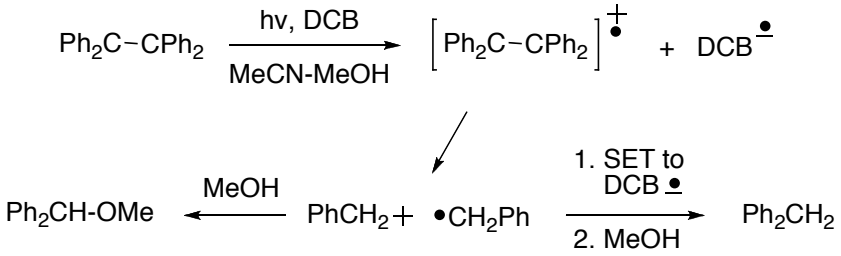

Importantly, no products arising via reduction of radical **21** (Scheme 6) by $DCA^{-\bullet}$ are formed in the DCA photoinduced reactions of **1T** and **1E**. Instead, **21** is transformed to the diol **5** and α-hydroxyketone **6**. The former substance arises

by oxidation of **10** through SET to DCA or H-DCA• followed by water addition to the resulting cation. In contrast, α-hydroxyketone **6** might arise by addition of adventitious dioxygen to **10** or addition of superoxide ($O_2^{-\bullet}$), produced by reaction of dioxygen with $DCA^{-\bullet}$. The observation that **6** becomes a major product when photoreactions of **1T** and **1E** are carried out in dioxygen saturated solutions supports these proposals for its origin.

UV-spectroscopic monitoring of the reactions of **1T** and **1E** in N_2 saturated solutions shows that DCA is consumed. However, this is not the case for the corresponding reactions in dioxygen saturated solutions (see Figure S4 in Supporting Information). The disappearance of DCA under the N_2 saturated conditions is responsible for the low conversions seen in the photoreactions and is consistent with the proposal that diol **5** forms by SET from **10** to DCA or HDCA•. The effect of dioxygen in facilitating DCA-promoted photoreactions of the lignin model compounds (see Table 1) is attributable to its ability to oxidize $DCA^{-\bullet}$ or HDCA•, which results in regeneration of DCA. However, in light of a number of early studies, which were directed at probing singlet oxygen ($O_2^{\,S_1}$) promoted oxidative cleavage reactions of lignin[61-64] and lignin model compounds,[65] it is necessary to consider an alternative manner by which O_2 participates in these photoreactions. Although mechanistically difficult to rationalize, it is possible that when oxygen is present in reasonably high (*ca* 3 mM in O_2 saturated solutions) concentrations, the conversion of the β-1 lignin model compounds to VAD, diol **5** and ketoalcohol **6** might be promoted by $O_2^{\,S_1}$. However, based on the results of

more recent investigations,[66-68] perhaps most notably the one carried out by Eriksen and Foote,[67] along with a consideration of (1) substrate versus oxygen concentrations, (2) rates of SET from the models versus energy transfer from O_2 to DCA ^{S_1}, and (3) chemical reasoning, it seems highly unlikely that O_2 ^{S_1} is formed to an appreciable extent in these reactions and that even if it were it would promote C-C bond cleavage processes.

The comparison of DCA-promoted photoreactions of the β-1 model compounds and DCB-photosensitized reactions of 1,1,2,2-tetraphenylethane and its derivatives is interesting. As pointed out above, in the DCB-promoted reactions studied earlier by Arnold and his coworkers, diphenylmethyl radicals formed by C-C bond cleavage reactions participate as electron acceptors in SET with $DCB^{\bullet -}$ (Scheme 7). In contrast, the dimethoxy-substituted benzyl radical **10**, paired with $DCA^{\bullet -}$, is instead oxidized to produce the cation precursor of diol **5**. Several factors might be responsible for this difference. Firstly, as a more stable anion radical $DCA^{\bullet -}$ is less prone to donate an electron to benzylic radicals. This property is reflected in the larger reduction potential of DCA (*ca* -0.9 V)[62] versus DCB (*ca* -1.7 V)[48] which indicates the relative stability and reducing ability of the corresponding radical anion. Secondly, although the reduction potential of the α-alkyl-dimethoxyphenyl substituted benzyl radical **10** is not known, it is predicted to be low and, thus, that the radical would be difficult to reduce. This is seen in the comparison of the known reduction potentials of the diphenylmethyl radical ($Ph_2\dot{C}$; -1.14 V)[67] versus that of the p-methoxycumyl radical (*p*-$MeOC_6H_4\dot{C}Me_2$,

-1.9 V)[74] which models **10**. Finally, the very low oxidation potentials of ring-methoxy and α-alkyl substituted benzyl radicals (*eg*. -0.14 for *p*-$MeOC_6H_4\dot{C}Me_2$)[67] suggest that **10** will have a much greater propensity to be oxidized than reduced.

A comment about the origin of β-hydroxyketone **7**, formed in DCA promoted photoreactions of **1T** (8%) and **1E** (trace), is in order. This substance most likely arises by loss of the C-1 benzyl protons from the initially formed cation radical intermediates. This common reaction pathway.[70] leads to formation of a benzylic radical, which following SET oxidation and loss of a proton yields **7**. The factors governing the relative rates of C-C and C-H bond cleavage in cation radicals related to $1^{+\bullet}$, will be discussed in more detail below.

Mechanistic pathways similar to those discussed above are involved in DCA promoted photoreactions of the β-O-4 model compounds **2E** and **2T**. In the β-O-4 radical cations, the charged radical center should be more highly localized on the C-1 aryl rather than 2-aryloxy ring (Scheme 8).[71] Carbon-carbon bond

Scheme 8.

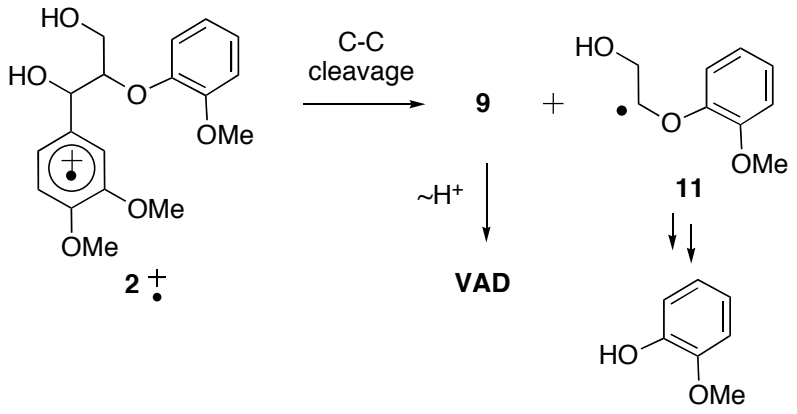

cleavage in these radical cations produces a radical cation pair in which the positive charge resides on the hydroxybenzylic component **9** and the radical on the aryloxyalkyl part **11**. Like in the pathway for reactions of the β-1 models, deprotonation of **9** forms VAD and an oxidation-hydrolysis sequence transforms **11** to guaiacol. Finally, the cation radicals derived from **2E** and **2T** also undergo benzylic deprotonation to yield precursors of the β-hydroxyketone **4**. Although, this is only a minor pathway followed in reactions of the β-1 models and the β-O-4 erythro isomer, loss of the C-1 benzylic proton from the cation radical of **2T** is highly competitive with C-C bond cleavage (see below).

Product Distributions. Despite the fact that different SET oxidants are involved and that widely different conditions are employed, the DCA, CAN and LP promoted reactions of the lignin model compounds produce remarkably similar product distributions. In almost all of these processes, C1-C2 bond cleavage products (*eg* VAD) predominate. To varying extents and depending on the nature of the model (β-1 vs. β-O-4) and stereochemistry (erythro *vs*. threo), β-hydroxyketone products arising by benzylic oxidations are also generated. Interesting in this regard are the DCA, CAN and LP promoted reactions of the diastereomeric β-O-4 models where benzylic oxidation is the minor (for **2E**) or major (for **2T**) route followed. For example, β-hydroxyketone **4** is formed in low yields (5-11%) in all types of oxidation reactions of **2E**. In comparison, this ketone and its nitro-derivative **8** are generated in yields ranging from 22-65% in oxidation reactions of **2T**. This difference is dramatized in the CAN reactions of **2E** and **2T**, where C-C bond cleavage (*i.e.* formation of VAD) dominates by 12:1

over benzylic oxidation in **2E** and becomes a minor process (1:2) in CAN oxidation of **2T**.

The difference observed in the nature of the dominant pathways followed in reactions of cation radicals arising from **2E** and **2T** (and to a lesser extent with **1E** and **1T**), are likely a consequence of stereoelectronic effects. As Arnold demonstrated earlier in investigations with phenylcyclopentane derivatives,[50] C1-C2, bond cleavage in cation radicals of 1-phenylethanes requires the availability of conformations in which the vulnerable C-C bond overlaps with the SOMO of the arene localized cation radical. When this requirement is not met and benzylic C-H SOMO overlap is preferred, deprotonation of the cation radical takes place. Thus, the source of the differences in the C-C vs C-H bond cleavage reactivity of the **2E** and **2T** cation radicals (and to a lesser extent with **1E** and **1T**) might be associated with a difference in C1-C2 bond conformational preferences in the two diastereomers. Although not being performed at a high level or on cation radicals and not including solvent effects, the results of AMI level calculations suggest that **2E** has a lowest energy conformation in which the C1-C2 bond is well overlapped with the π-system of the C-1 arene ring. In contrast, the C1-C2 bond in **2T** is less well aligned with the π-system of the C-1 arene ring (Figure 12). However, higher level calculations will be required to determine if cation radical conformations are the true source of the differences in product distributions arising from reactions of the β-O-4 model compounds.

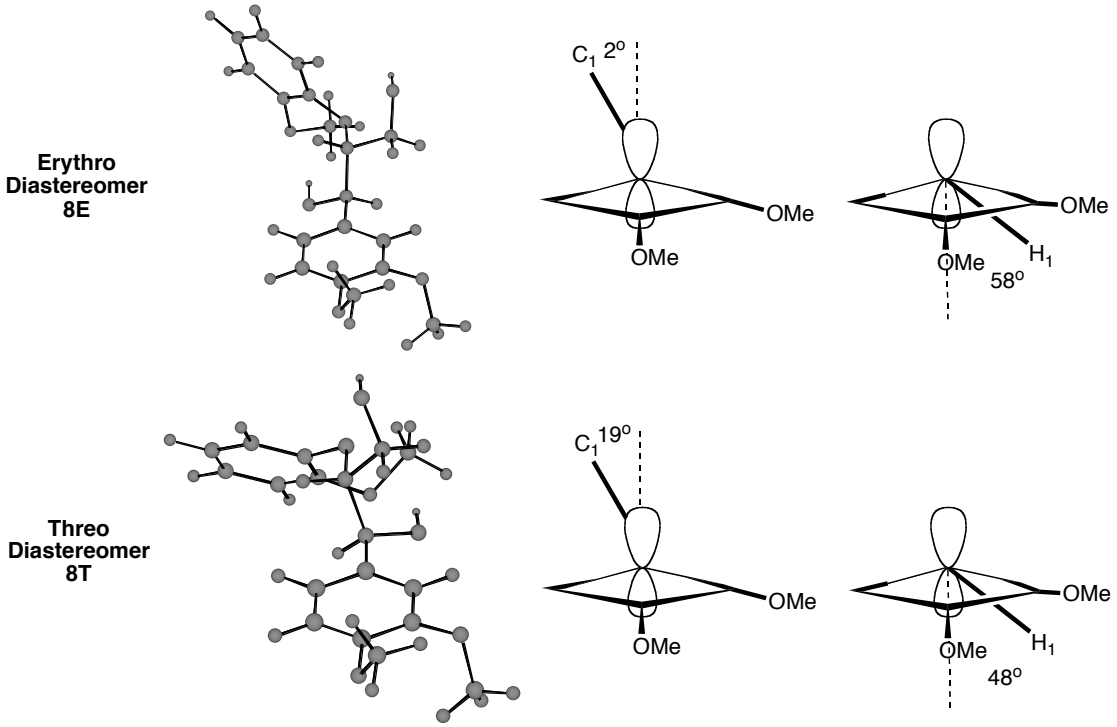

Figure 12. *Summary of AMI Calculated Lowest Energy Conformers of* ***2E*** *and* ***2T****.*

Additional observations made in reviewing the product distributions deserve brief comment. As mentioned above, the major products generated in the DCA, CAN and LP promoted reactions of the β-1 model compounds are VAD, diol **5** and ketoalcohol **6**. The latter two products arise from the C2-C3 fragment of each of the models. In contrast, oxidations of the β-O-4 models yield only small amounts of guaiacol, which also corresponds to a portion of the C2-C3 fragment. This finding, which matches those made by others in studies of enzymatic and non-enzymatic reactions of β-O-4 models (see above), is likely caused by the instability of guaiacol under oxidative conditions. Finally, the formation of nitroaryl ketone **8** in CAN oxidations of **2E** and **2T** is interesting.

This substance, arises by secondary oxidation of the initially formed ketone **4**. While arene nitration reactions of this type are well documented,[72] why the process occurs only in the case of the β-O-4 models and only on the aryloxy ring of the ketone and not starting substrate is difficult to understand.

Cation Radical C-C Bond Cleavage Rates. One of the main aims of our studies in this area is to determine how both structural (β-1 *vs*. β-O-4) and stereochemical (erythro *vs*. threo) features govern the C-C bond cleavage reactivities of cation radicals arising by SET oxidation of lignin model compounds. As described above, three different methods were employed to generate the cation radicals of the models and three different techniques were used to obtain C-C bond cleavage rate data. These include measurements of relative quantum yields of DCA-promoted photoreactions and the rates of CAN and LP induced oxidations. In order that the data coming from each of these experiments have meaning, account needs to be taken of how the measurement were made and, consequently, their relationship to cation radical C-C bond cleavage rates.

The relative quantum yields for VAD formation (Table 2) in the DCA-promoted photoreactions, determined under identical conditions and at low conversions should be directly proportional to the related rates of C-C bond cleavage. Specifically, when equivalent concentrations of DCA and each lignin model are used in simultaneous irradiation experiments, equivalent numbers of photons are absorbed by DCA and an equivalent fraction of DCA^{S_1} are being quenched by SET from the lignin models when corrections are made using the k_q

values given in Table 2. Cation radicals produced in the SET step can undergo C-C bond cleavage to form VAD along with highly exothermic back electron transfer (BSET) to $DCA^{\bullet -}$. Consequently, differences in the quantum yields for VAD formation are directly related to differences in the rate constants for cation radical C-C bond cleavage. The relative C-C bond cleavage rates, obtained from an analysis of the relative quantum yield data and correcting for differences in the rates for DCA^{S_1} quenching, are given in Table 7.

Table 7. Relative Rates of C-C Bond Cleavage in Cation Radicals Arising from SET-Oxidation of Lignin Model Compounds.

	Relative Rates		
Model	From DCA Promoted Reactions	From CAN Promoted Reactions	From LP Promoted Reactions
1T	5	25	53
1E	7	11	123
2E	2	4	1
2T	1	1	1

The rate constants determined for CAN promoted oxidations of the lignin models are based on the rates of CAN disappearance. Consequently, they only partially reflect the rates of cation radical C-C bond cleavage owing to the fact that the observed rates also represent a complex function of the rates of SET from the models to Ce(IV) and of BSET as well as other oxidation reactions (*e.g.* benzylic

oxidation). Employing the reasonable assumption that both the SET and BSET rates will be the same for each model compound, the observed rates given in Table 4 are directly proportional to C-C bond cleavage rates if account is taken for the proportion of competitive benzylic oxidation taking place. This is especially true in the case of the β-O-4 models **2E** and **2T** where a significant fraction of the process involves benzyl C-H rather than C1-C2 bond cleavage. Since the CAN oxidation kinetic measurements were made at very short reaction times and correspondingly low conversion, correction for the formation of both **1** and **8**, both arising by benzylic oxidation, does not have to be performed separately. Thus, after correcting for competitive formation of **1** + **8** from **2E** and **2T**, the averages of the rate data in Table 4 become the relative cation radical C-C bond cleavage rates listed in Table 7.

Finally, owing to the method used for kinetic analysis, k_{cat} values for LP catalyzed reactions of the lignin models correspond to the formation of all products that absorb at 310 nm. Thus, in order to determine the rates of C-C bond cleavage which yields VAD, the extinction coefficients at 310 nm of VAD (1.06×10^4) and ketoalcohols **6** (0.95×10^4) and **4** (1.06×10^4) along with the relative amounts of each substance produced in the LP promoted processes must be considered. Treatment of the k_{cat} values in Table 6 in this manner yields the relative rates of cation radical C-C bond cleavage derived from analysis of the kinetics of enzymatic reaction given in Table 7.

Summary of Rate Data. The relative rate data arising from kinetic analyses of the DCA, CAN and LP-promoted reactions contain several

interesting features related to the cation radical C-C bond cleavage process. Firstly, although stereochemistry of the β-1 and β-O-4 compounds definitely influences bond cleavage rates, the trends vary depending on the oxidation conditions employed. For example, the cation radical of the erythro diastereomer of the β-1 model **1E** is transformed more rapidly to VAD under the conditions used in the DCA photochemical and LP catalyzed reactions. In contrast, the threo isomer **1T** is more reactive than **1E** in CAN-promoted reactions. Likewise, the β-O-4 erythro isomer **2E** undergoes C-C bond cleavage more rapidly than the threo analog **2T** under both DCA and CAN conditions, **2E** and **2T** are about equally reactive in the LP catalyzed process.

It should be noted that the results of earlier studies[73-76] of metal oxidation and LP reactions, although mixed,[77] showed that the rates of disappearance of **2T** exceeds that of **2E**. However, to our knowledge in no previous effort have the relative rate data been adjusted to account for the fact that **2T** reacts by competitive C-C and C-H bond cleavage pathways to produce VAD and ketoalcohol **4**, respectively. When this fact is taken into account, the rates of C-C bond cleavage of the **2E** cation radical becomes larger than or near equal to that of the **2T** cation radical.

The most significant observation made in the current investigation is that, independent of the method used and their stereochemistry, cation radicals derived from the β-1 lignin models undergo C-C bond cleavage at rates that far exceed those of the β-O-4 models. The β-1:β-O-4 rate ratios range from 7:1 to 123:1 when the most reactive *vs.* least reactive stereoisomer in each series is

compared. This finding has both mechanistic and potentially practical significance.

Analysis of Rates. As has been discussed earlier by Arnold, Maslak and others, the reactivity of radical cations generated by SET oxidation of substituted 1,2-diarylethanes and 1-aryl-2-ethyl ethers appears to be governed by cation radical C-C bond dissociation energies (BDEs) and conformations. With some simple aryl substituted ethanes, it is possible to calculate or estimate radical cation BDEs by using simple thermochemical cycles[46] like the one shown in Figure 13. In these cycles, the

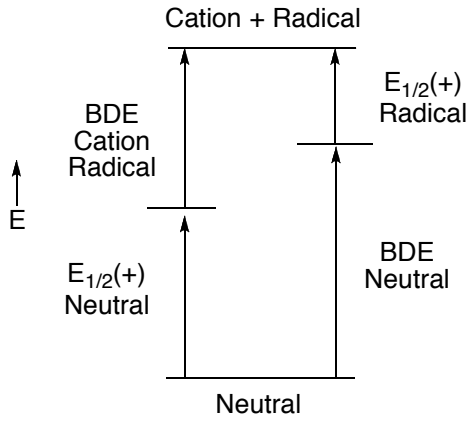

Figure 13. *Thermochemical cycle to calculate C-C bond dissociation energies of diarylethanes and arylethyl ethers.*

energy required to produce the radical cation pair is comprised on one hand of the BDE of the neutral substrate and the oxidation potential of the more easily oxidized radical product and, on the other hand, of the oxidation potential of the substrate and the BDE of the cation radical. Consequently, knowing the

substrate oxidation potential and C-C BDE and $E_{½}(+)$ of the most easily oxidized radical, it is possible to calculate the cation radical BDE. Unfortunately, in spite of the detailed studies by Griller and Wayner,[58-60] only a small number of radical oxidation potentials are known. In addition, C-C BDEs of highly substituted diarylethanes and arylethyl ethers have not been determined. Thus, insufficient information is available to determine the cation radical BDEs of the β-1 and β-O-4 models.

The situation is further complicated by inspection of reactivity profiles of substances that might be considered as simple models of the β-1 (diarylethanes) and β-O-4 (arylethyl ethers) models. Accordingly, Arnold[46] showed that in contrast to 1,1,2-triphenylethane, whose SET generated cation radical is unreactive, the 1,1-diphenyl-2-ethyl ether cation radical undergoes smooth C-C bond cleavage. Based on this observation, one might predict that cation radicals arising from the β-O-4 substrates (complex arylethyl ethers) would undergo C-C bond cleavage more readily than those of the β-1 models (complex diarylethanes). However, a consideration of roughly estimated thermochemical cycles suggest that the C-C BDEs of β-1 cation radicals should be lower than those of their β-O-4 counterparts. Specifically, since the oxidation potentials of the β-1 and β-O-4 model compounds are roughly equal and the same radical is oxidized to form the cationic intermediate **9** in both thermochemical cycles, the relative cation radical BDEs of the β-1 and β-O-4 compounds should be directly related to the BDEs of the neutral substrates. Although the values are not known, the BDEs of the simple analogs, 1,2-diphenylethane (64 kcal/mol)[77] and 1-

phenylethyl phenyl ether (77 kcal/mol),[78] have been calculated. This comparison suggests that the cation radical BDEs of the β-1 compounds should be lower than those of the β-O-4 analogs. Clearly, contributions made by methoxy substituents on the arene rings and the hydroxyl and hydroxymethyl groups found in **1** and **2** need to be considered in this analysis since they should have profound impacts on cation radical C-C bond dissociation energies.

Experimental

General.

Stock Solutions, Tartrate Buffer. To a 500 mL volumetric flask containing approximately 200 mL of deionized water was added 3.68 g tartaric acid was added. To this solution was added 5.86 g sodium tartrate. The pH was found to be 3.37.

Enzyme Stock Solution. Lignin peroxidase (LP) was purchased from Sigma-Aldrich (9.7 U/mg) and used without further purification. Using 0.1 M tartrate buffer at pH 3.4, 30 mg of dried enzyme was added to 15 mL of buffer and the resulting solution was gently agitated and filtered. Enzyme stock solutions (2 mg/mL) were kept on ice throughout each experiment.

Substrate Stock Solution. Stock solutions containing each of the lignin model compounds of 0.1 M concentrations in methanol were prepared and kept at room temperature during experiments to avoid precipitation.

Hydrogen Peroxide Stock Solution. Twenty six uL of 30% hydrogen peroxide was diluted with water to yield a 0.025 M solution and was stored in a

vial wrapped in aluminum foil to avoid photodegradation.

HPLC Method

HPLC analyses were performed by using a Restek Ultra Aqueous C-18 reverse phase column (250 mm length, 5 μm particle size , 100 Å pore size, 4.6 mm inner diameter) with water-methanol gradient (starting with 20 % methanol and ending with a sweep of 80 % methanol, with holds at 40 % and 60 % methanol, and a total run time of 60 min) as the mobile phase. A reaction profile was established for each method of degradation by retention time comparison to commercially available or synthesized compounds and confirmed by NMR analysis. A calibration curve was run, varying concentrations of all compounds from 20 uM to 1500 uM. The product yields were then determined by area comparison.

Veratryl Alcohol Assay of LP. The time dependence of the veratryl alcohol (VA) oxidative conversion to veratryl aldehyde (VAD) was determined by reacting LiP with 4000 uM VA and 83 uM hydrogen peroxide in tartrate buffer, and quenching with 12 uL 2.5 M potassium hydroxide at reaction times ranging from 2-40 min. The resulting mixtures were analyzed by using HPLC. The areas of the peaks corresponding to VAD were plotted versus time.

Determination of LP, Hydrogen Peroxide and Substrate 1E, 1T, 2E and 2T Concentration Dependences of C-C Bond Cleavage Reactions of the Lignin Model Compounds. **Enzyme.** Solutions containing 100 μM hydrogen peroxide, 200 μM of the lignin model compound **1E, 1T, 2E** and **2T**, and 0.24 - 0.48 μM of LP were examined. The progress of each reaction was monitored by measuring the absorbance increase at 310 nm. As LP concentration is

increased, the rate of product formation increased. However, product formation ceased in all cases prior to complete consumption of the substrate.

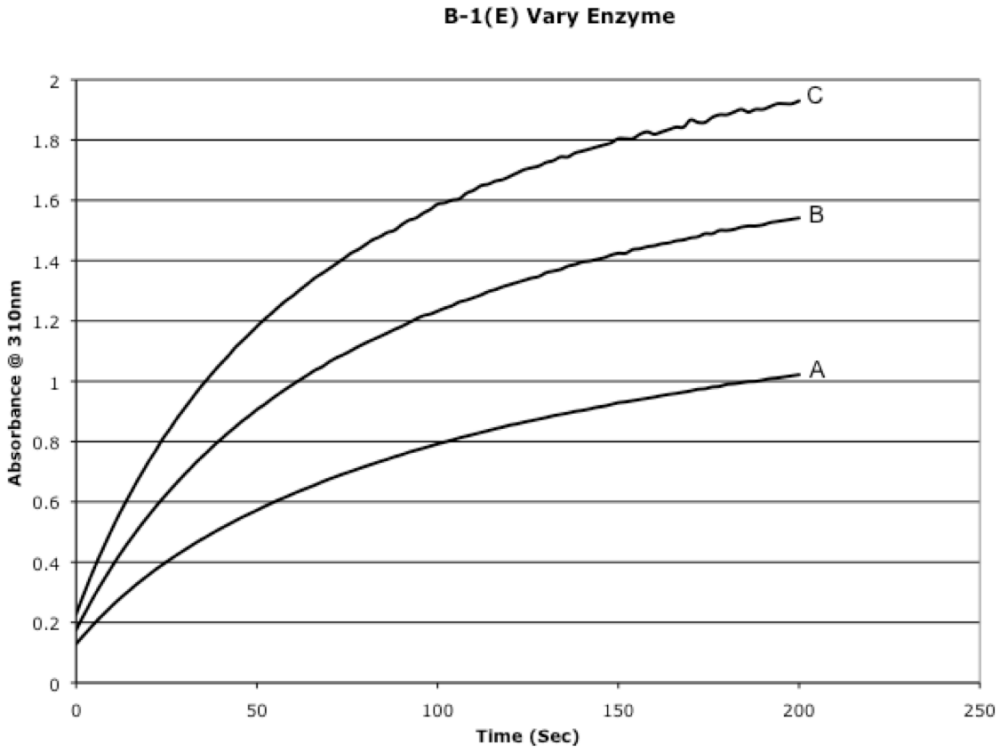

Figure 14. *Plots of absorbances vs. time for LP catalyzed reactions of* ***1E*** *to generate VAD using 200 uM 1E, 100 uM* H_2O_2 *and (A) 0.24 uM LP, (B) 0.36 uM LP, (C) 0.48 uM LP.*

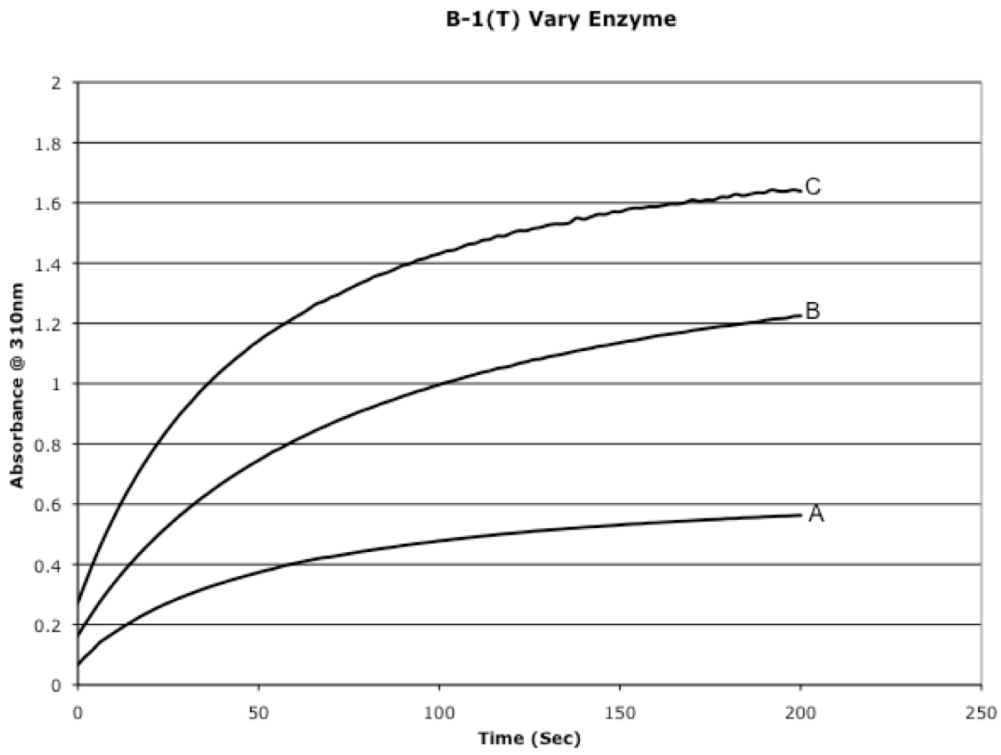

Figure 15. *Plots of absorbances vs. time for LP catalyzed reactions of* ***1T*** *to generate VAD using 200 uM 1E, 100 uM H_2O_2 and (A) 0.24 uM LP, (B) 0.36 uM LP, (C) 0.48 uM LP.*

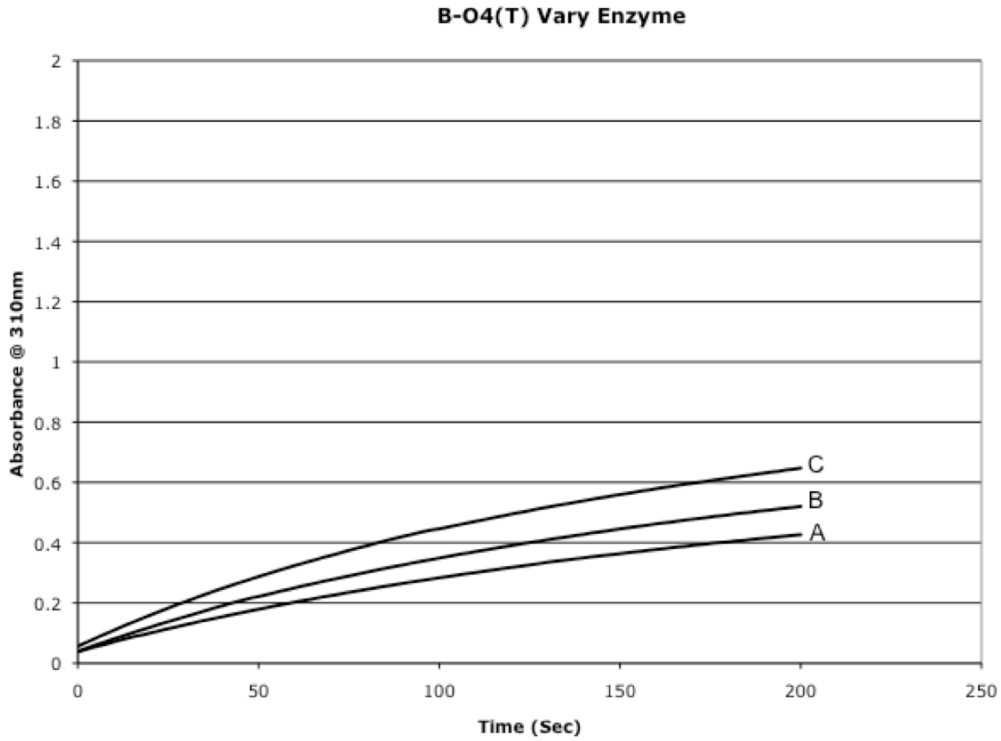

Figure 16. *Plots of absorbances vs. time for LP catalyzed reactions of* ***2T*** *to generate VAD using 200 uM 1E, 100 uM H_2O_2 and (A) 0.24 uM LP, (B) 0.36 uM LP, (C) 0.48 uM LP.*

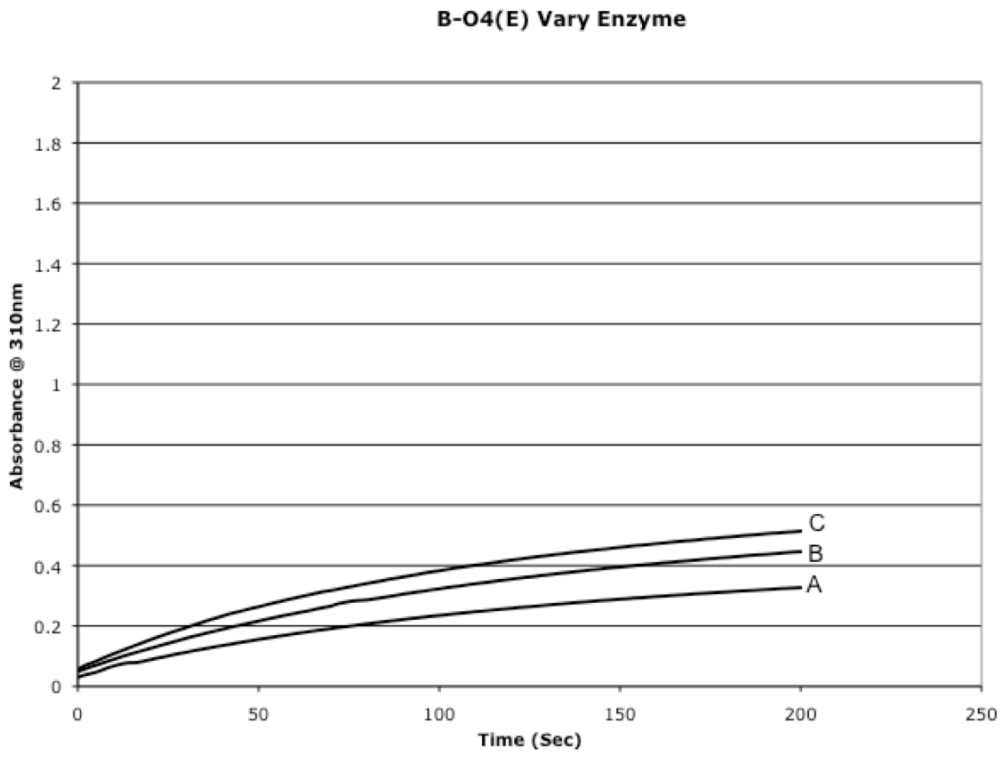

Figure 17. *Plots of absorbances vs. time for LP catalyzed reactions of 2**E** to generate VAD using 200 uM **1E**, 100 uM H_2O_2 and (A) 0.24 uM LP, (B) 0.36 uM LP, (C) 0.48 uM LP.*

Substrate. Solutions containing 200 μM hydrogen peroxide, from 100 - 300 μM of a mixture of the lignin model compound **1E** and **1T**, and 0.48 μM of LP were examined. The progress of each reaction was monitored by measuring the absorbance increase at 310 nm. The results show that when substrate concentrations are below that of hydrogen peroxide the initial absorbance change, which relates to the overall activity of the system, are substantially lower than those observed when substrate concentrations are equal to or greater than the hydrogen peroxide concentration.

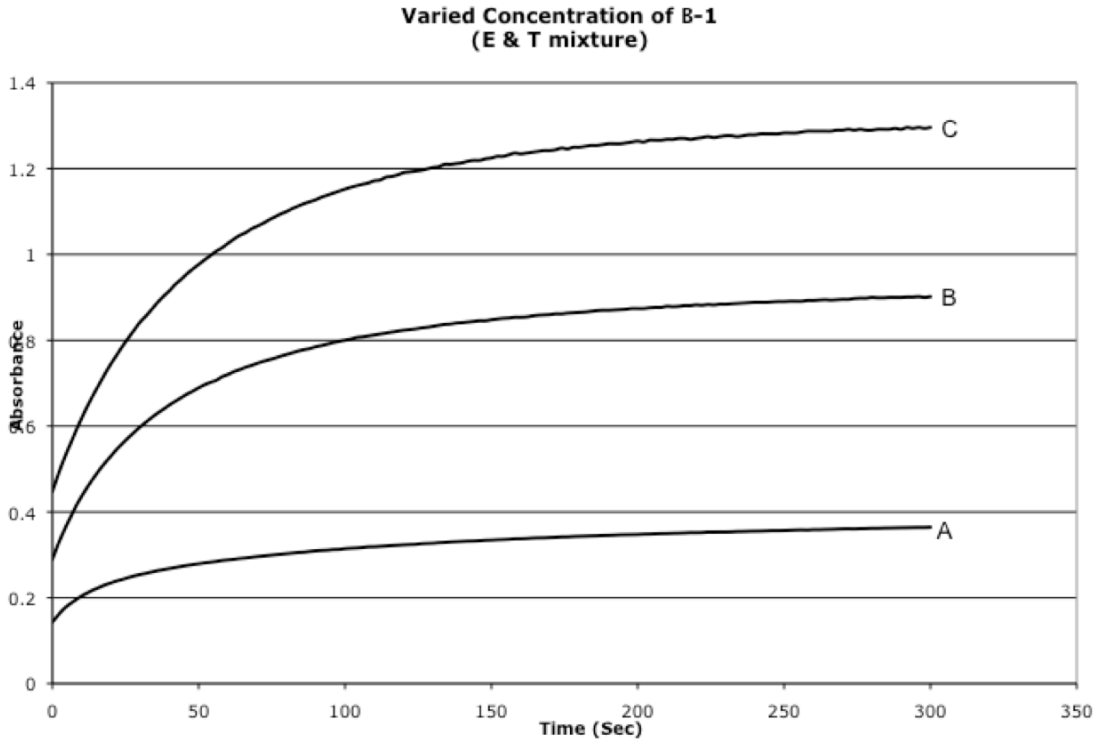

Figure 18. *Plots of absorbances vs. time for LP catalyzed reactions of a mixture of* ***1E*** *and* ***1T*** *to generate VAD using (A) 100 uM* ***1E*** *&* ***1T,*** *(B) 200 uM* ***1E*** *&* ***1T****, and (C) 300 uM* ***1E*** *&* ***1T,*** *with 100 uM* H_2O_2*, and 0.48 uM LP.*

Hydrogen Peroxide. In these experiments, both the hydrogen peroxide and lignin model compound concentrations were varied and the concentration of LP was 0.36 μM in all cases. The substrate **1E, 1T, 2E** and **2T**/hydrogen peroxide concentrations were varied in the following manner 400 μM/0 μM; 50 μM/100 μM; 50 μM/50 μM; 100 μM/100 μM; 200 μM/200 μM; 400 μM/400 μM; 200 μM/100 μM; and 400 μM/100 μM. The results show that at low substrate to peroxide concentrations, the activity of the system is low.

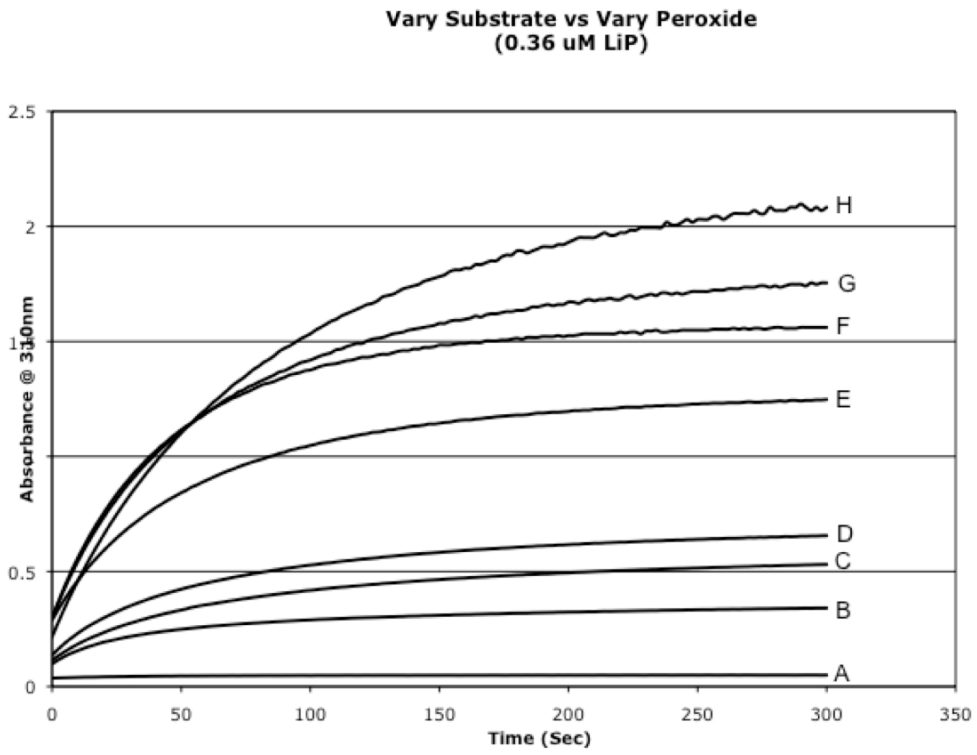

Figure 19. *Plots of the absorbances vs. time of LP catalyzed reactions of a mixture of* ***1E*** *and* ***1T*** *to generate VAD using (A) 400 uM* ***1E*** *&* ***1T*** *and 0 uM H_2O_2, (B) 50 uM* ***1E*** *&* ***1T*** *and 100 uM H_2O_2 (C) 50 uM* ***1E*** *&* ***1T*** *and 50 uM H_2O_2, (D) 100 uM* ***1E*** *&* ***1T*** *and 100 uM H_2O_2, (E) 200 uM* ***1E*** *&* ***1T*** *and 200 uM H_2O_2, (F) 400 uM* ***1E*** *&* ***1T*** *and 400 uM H_2O_2, (G) 200 uM* ***1E*** *&* ***1T*** *and 100 uM H_2O_2, and (H) 400 uM* ***1E*** *&* ***1T*** *and 100 uM $H_2O_2$with 0.36 uM LP.*

In another experiment, mixtures containing 0.36 μM LP, 200 μM lignin model compound **1E, 1T, 2E** and **2T** and hydrogen peroxide concentrations varying from 12.5 – 200 μM. The absorbance change at 310 nm was found to increase as the hydrogen peroxide concentration increased but the absorbance increase reached a constant value at high hydrogen peroxide concentrations.

The observations led to the decision to use a hydrogen peroxide concentration of 100 μM in steady state kinetic enzyme assays and 50 μM in stopped flow assays (see below).

Lignin Peroxidase Catalyzed Reactions of 1E, 1T, 2E and 2T. To 0.968 mL of 0.1 M tartrate buffer (pH 3.4) were added 10 μL of each substrate **1E, 1T, 2E** and **2T** (0.1 M, final concentration 200 μM) and 8 μL of H_2O_2 (1.25 x 10^{-2} M, final concentration 100 μM). After adding 15 μL of lignin peroxidase (0.15 unit, 0.36 μM) the solutions were agitated for 10 min and then subjected to HPLC analysis to yield the following products from **2E** (35 % conversion): VAD (35 %), **3** (trace) and **4** (4 %); from **2T** (66 % conversion): VAD (31 %), **3** (trace) and **4** (29 %); from **1T** (73 % conversion): VAD (52 %), **5** (trace) and **6** (14 %); from **1E** (77 % conversion): VAD (45 %), **5** (trace) and **6** (15 %).

Lignin Peroxidase Reactivity of 1E, 1T, 2E and **2T**. To 1 mL cuvettes, 0.968 mL of 0.1 M tartrate buffer (pH 3.4), 10 μL each of **1E, 1T, 2E** and **2T** (0.1 M, final concentration 200 μM) and 8 μL of H_2O_2 (1.25 x 10^{-2} M, final concentration 100 μM) were added. The reactions were initiated by addition of 15 μL of lignin peroxidase (0.15 unit, 0.36 μM) to each cuvette. The progress of each reaction was monitored by following the rise in absorbance 310 nm, corresponding to formation of VAD and (3.75 x 10^{-4} M) over 5-200 s periods. The results are displayed in Figure 7.

In a stopped flow apparatus, solutions of LP (3.6 μM) in tartrate buffer (pH 3.4) containing H_2O_2 (100 μM) were mixed with solutions containing 100, 200, 300, 400 and 500 μM of **1E, 1T, 2E** and **2T**. The absorbance increases at 310

nm, corresponding to the formation of VAD and keto-alcohols **6**, **7** (for **1T** and **1E**) and **4** (for **2E** and **2T**) were measured over a 0.1-1 s time period. The ΔA_{310} values were converted to concentration changes (ΔC_{VAD}) and reaction rates (v) by using the following equations: $\Delta C_{VAD} = \Delta A / \varepsilon_{VAD,310nm}$ and $v = \Delta C$ / time. Plots of the rates of these processes versus substrate concentration and the corresponding Lineweaver Burke plots of 1 / v versus 1 / [S] are given in Figures 20 and 21.

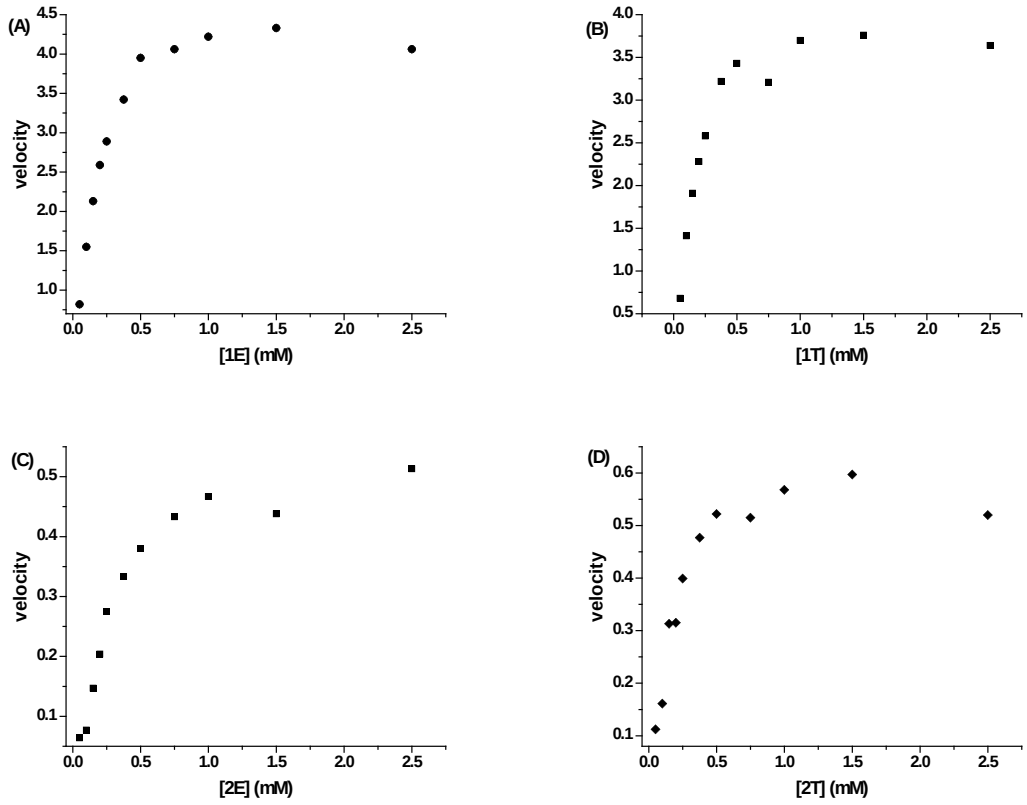

Figure 20. *Plots of the rates of LP promoted formation of VAD and keto-alcohols **6**, **4** and **7** as a function of the concentrations of **1E, 1T, 2E** and **2T**.*

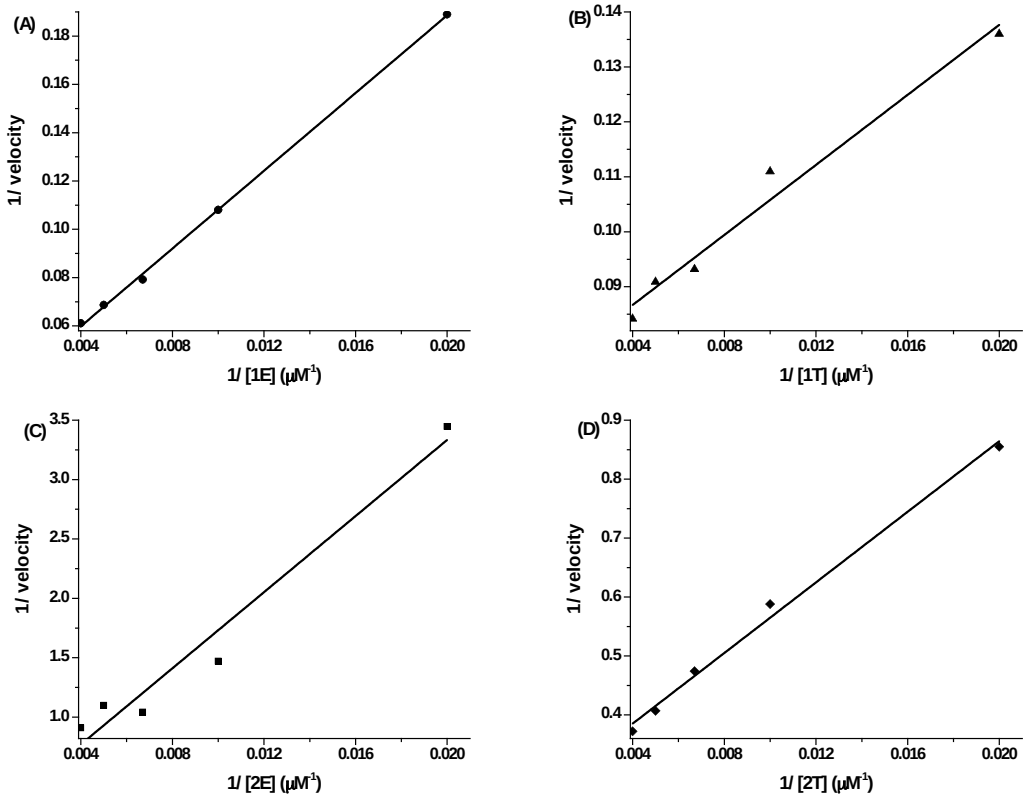

Figure 21. *Lineweaver Burke plots of the reciprocals of the rates of LP promoted formation of VAD and keto-alcohols* ***6****,* ***4*** *and* ***7*** *versus the reciprocals of the concentrations of* ***1E, 1T, 2E*** *and* ***2T*** *in LP.*

CAN Reactions of 1E, 1T, 2E and **2T.** Individual solutions containing the substrates **1E, 1T, 2E** and **2T** (2.0 mg, 6.0 x 10^{-6} mol) and CAN (6.6 mg, 1.2 x 10^{-5} mol) in 12 mL of MeCN were stirred for 15 h at room temperature (90%, 96%, 100% and 100% conversions of the respective substrates). The resulting

mixtures were concentrated in *vacuo* and subjected to HPLC analysis to yield from **2E**: VAD (88 %), **3** (trace), **4** (7 %) and **8** (4 %); from **2T**: VAD (31 %), **3** (trace), **4** (32 %) and **8** (33 %); from **1T**: VAD (95 %), **6** (25 %) and **7** (trace); from **1E**: VAD (95 %), **6** (46 %) and **7** (trace).

8: ^{1}H-NMR 3.91 (s, 3H, OCH_3), 3.92 (s, 3H, OCH_3), 3.95 (s, 3H, OCH_3), 4.09-4.17 (m, 2H, CH_2), 5.60-5.62 (m, 1H, CH), 6.90-6.94 (m, 2H, aromatic), 7.56 (d, 1H, *J* = 2 *Hz*, aromatic), 7.69-7.71 (m, 2H, aromatic), 7.92-7.94 (m, 1H, aromatic); ^{13}C-NMR 29.7, 56.0, 56.2, 56.4, 63.7, 83.1, 110.2, 110.8, 110.9, 111.7, 119.5, 123.4, 127.6, 141.2, 146.6, 149.5, 154.4, 155.5, 193.3; HRMS (ES) *m/z* 400.1008 (M+Na, $C_{18}H_{19}NO_8Na$ requires 400.1004)

CAN reaction of 4. A 50 mL MeCN solution containing **4** (300 mg, 0.9 mol) and CAN (1.0 mg, 1.8 mmol) was stirred for 13 h at room temperature (ca. 60 % conversion of **4**). The resulting mixture was concentrated in *vacuo* and the residue was subjected to column chromatography to yield 187 mg (55 %) of **8**.

CAN Reactivity of 1E, 1T, 2E and **2T**. The absorbances at 400 nm of independent solutions of **1E, 1T, 2E** and **2T** (1.25×10^{-4} M) containing CAN (2.5×10^{-4} M) in 3.0 mL of MeCN were monitored 5 s after mixing. A plot of Absorbance versus time is shown in Figure 11.

In a stopped flow apparatus, MeCN solutions of CAN (3.0×10^{-4} M) were added to solutions containing six different concentrations of **1E, 1T, 2E** and **2T** (7.5×10^{-5}, 3.75×10^{-5}, 1.5×10^{-5}, 7.5×10^{-6}, 3.75×10^{-6} M). Changes in absorbances at λ_{390} (for CAN, λ_{390nm} = 2840) of these solutions over a 0.1-0.25 s period were monitored. From plots of time versus absorbance, initial slopes

corresponding to ΔA_{390} versus t (0.1-0.25 s) of each reaction were obtained. These ΔA_{390} values were converted to concentration changes (ΔC_{lignin}) and reaction rates (v) of each reaction were determined by using the following equations: $\Delta C = \Delta A_{CAN} / 2\varepsilon_{390nm}$ and $v = \Delta C_{lignin} / 0.5$. From plots v versus concentrations (Figure 12), the rate constants (k) CAN reaction of each compound was determined (Table 4).

In a stopped flow apparatus, MeCN solutions of **1E, 1T, 2E** and **2T** (3.75×10^{-4} M) containing six different concentrations of CAN (1.5×10^{-4}, 1.80×10^{-4}, 2.10×10^{-4}, 2.40×10^{-4}, 3.00×10^{-4}, and 3.60×10^{-4} M). Changes in absorbances at λ_{390} (for CAN, $\lambda_{390nm} = 2840$) of these solutions over a 0.1-0.25 s period were monitored. From plots of time versus absorbance, initial slopes corresponding to ΔA_{390} versus t (0.1-0.25 s) of each reaction were obtained. These ΔA_{390} values were converted to concentration changes (ΔC_{CAN}) and reaction rates (v) of each reaction were determined by using the following equations: $\Delta C = \Delta A_{CAN} / 2\varepsilon_{390nm}$ and $v = \Delta C_{lignin}$. From plots of v versus concentrations (Figure 12), the rate constants CAN reaction of each compound was determined (Table 4).

References

1. ten Have, R.; Teunissen, J. M., *Chem. Rev*., **2001**, 101, 3397-3413

2. US Department of Agriculture and US department of Energy, *Biomass as a Feedstock for a Bioenergy and Bioproducts Industry: The Technical Feasibility of a Billion-Ton Annual Supply (US DOE, Oak Ridge, TN and US Department of Commerce, Springfield, VA, 2005)* http://www1.eere.energy.gov/biomass/pdfs/final_billionton_vision_report2.pdf

3. Wang, M.; Wu, M.; Huo, H., *Environ. Res. Lett.*, **2007**, 2, 024001

4. http://www.novozymes.com/en/MainStructure/PressAndPublications/PressRelease/2010/New+enzymes+turn+waste+into+fuel.htm

5. http://www.research.ufl.edu/publications/explore/v04n1/exchange.html

6. Yang, Q.; Zhan, H.; Wang, S.; Fu, S.; Li, K., *Bioresources*, **2007**, 2:4, 682-692

7. In Biology of Plants, 6th edition, Raven. P.H.; Evert, R.F.; Eichhorn, S.E.; *W.H. Freeman*, **1999.**

8. In Analytical Methods in Wood Chemistry, Pulping, and Papermaking (Springer Series in Wood Science), ed Sjöström, E; Alén, R., *Springer* **1999.**

9. Adler, E., *Wood Sci. Tech.*, **1977**, *11*, 169-218.

10. Keating, J.D.; Panganiban, C.; Mansfield, S.D., *Biotechnology and Bioengineering*, **2006**, 93:6, 1196-1206

11. Hu, W. J.; Kawaoka, A.; Tsai, C. J.; Lung, J.; Osakabe, K.; Ebinuma, H.; Chiang, V. L., *Proc. Nat. Acad. Sci.*, **1998**, *95*, 5407-5412

12. Ralph, J.; MacKay, J. J.; Hatfield, R. D.; O'Malley, D. M.; Whetten, R. W., *Science*, **1997**, *277*, 235-239.

13. Ralph, J.; Kim, H.; Peng, J.; Lu, F., *Org. Lett.*, **1999**, *1*, 323-326.

14. Grabber, J. H., *Crop Sci.*, **2005**, *45*, 820-831.

15. Meyer, K.; Cusamano, J. C.; Sammerville, C.; Chapple, C., *Proc. Natl. Acad. Sci.*, **1998**, *95*, 6619-6623.

16. Chen, F.; Dixon, R.A., *Nature Biotechnology, **2007,*** 25(7), 759-761

17. Chen, F,; Yasuda, F., *Planta,* **1999**, 207, 597-603.

18. Geib, S. M.; Filley, T. R.; Hatcher, P. G.; Hoover, K.; Carlson, J. E.; Jimenez-Gasco, M. dM.; Nakagawa-Izumi, A.; Sleighter, R. L.; Tien, M., *Proc. Nat. Acad. Sci.*, **2008**, *105*, 12932-12937.

19. Blumer-Schuette, S. E.; Kataeva, I.; Westpheling, J.; Adams, M. W.; Kelly, R. M., *Current Opinion in Biotechnology*, **2008**, *19*, 210-217.

20. Martínez, A. T.; Speranza, M.; Ruiz-Dueñas, F. J.; Ferreira, P.; Camarero,

S.; Martínez, M. J.; Gutíerrez, A.; del Río, J.C, *International Microbiology*, **2005**, 8, 195-204.

21. Hammel, K.; Cullen, D., *Current Opinion in Plant Biology*, **2008**, 11, 349-355.

22. Johjima, T.; Itoh, N.; Kabuto, M.; Tokimura, F.; Nakagawa, T.; Wariishi, H.; Tanaka, H., *Proc. Nat. Acad. Sci.*, **1999**, 96, 1989-1994.

23. Tien, M.; Kirk, T. K., *Science*, **1983,** *221*, 661-663.

24. Hammel, K. E.; Jensen, Jr., K. A.; Mozuch, M. D.; Landucci, L. L.; Tien, M.; Pease, E. A., *J. Biol. Chem.*, **1993**, *268*, 12274-12281.

25. Kirk, T. K.; Farrell, R. L., *Annu. Rev. Microbiol.*, **1987**, *41*, 465-501.

26. Ruiz-Dueñas, F. J.; Pogni, N.; Morales, M.; Giansanti, S.; Mate, M. J.; Romero, A.; Martínez, M. J.; Basosi, R.; Martínez, A. T., *J. Biol. Chem*, **2009**, 284:12, 7986-7994.

27. Doyle, W. A.; Blodig, W.; Veitch, N.C.; Piontek, K.; Smith, A.T., *Biochemistry*, **1998**, 37, 15097-15105.

28. Poulos, T.L.; Edwards, S. L.; Wariishi, H.; Gold, M. H., *J. Biol. Chem.*, **1993**, 268:6, 4429-4440.

29. Renganathan, V.; Gold, M. H., *Biochemistry*, **1986**, *25*, 1626-1631.

30. Hammel, K. E.; Tien, M.; Kalyanaraman, B.; Kirk, T. K., *J. Biol. Chem.*, **1985**, *260*, 8348-8353.

31. Kirk, T. K.; Tien, M.; Kersten, P. J.; Mozuch, M. D., *Biochem. J.*, **1986**, *236*, 279-287.

32. Marquez, L.; Wariishi, H.; Dunford, H. B.; Gold, M. H., *J. Biol. Chem.*, **1988**, *263*, 10549-10552.

33. Andrawis, A.; Johnson, K. A.; Tien, M., *J. Biol. Chem.*, **1988**, *263*, 1195-1198.

34. Wariishi, H.; Gold, M. H., *FEBS Lett*., **1989**, 243:2, 165-168

35. Tien, M.; Kirk, T. K., *Proc. Natl. Acad. Sci. USA*, **1984**, *81*, 2280-2284.

36. Kuwahara, M.; Glenn, J. K.; Morgan, M. A.; Gold, M. H., FEBS Lett., **1984**,

169, 247-250.

37. Glenn, J. K.; Gold, M. H., *Archives of Biochemistry and Biophysics*, **1985**, 242, 329-341.

38. Paszcynski, A.; Hyunh, V. B.; Crawford, R. L., *REMS Microbiol. Lett.*, **1985**, 29, 37-41.

39. Gold, M. H.; Glenn, J. K.; Mayfield, M. B.; Morgan, M. A.; Kutsuki, H. in Recent Advances in Lignin Biodegradation Research. **1983**, Tokyo Univ., pp 219-239.

40. Edwards, S. L.; Raag, R.; Wariishi, H.; Gold, M. H., *Proc. Natl. Acad. Sci. USA*, **1993**, 90, 750-754.

41. Poulos, T. L., *J. Biol. Chem*., **1997**, 272, 17574.

42. Khindaria, A.; Yamazaki, I.; Aust, S. D., *Biochemistry*, **1996**, 35, 6418-6424.

43. Trahanovsky, W. S.; Brixius, D. W., *J. Am. Chem. Soc*., **1973**, 95, 6778.

44. Davis, H. F.; Das, P. K.; Reichel, L. W.; Griffin, G. W., *J. Am. Chem. Soc.*, **1984**,106, 6968.

45. Arnold, D. R.; Maroulis, A. J., *J. Am. Chem. Soc.,* **1976**, 98, 5931.

46. Arnold, D. R.; LaMont, L. J., *Can. J. Chem*., **1989**, 67, 2119.

47. Okamoto, A.; Snow, M. S.; Arnold, D. R., *Tetrahedron*, **1986**, 42, 6175.

48. Okamoto, A.; Arnold, D. R., *Can. J. Chem*., **1985**, 63, 2340.

49. Popielarz, R.; Arnold, D. R., *J. Am. Chem. Soc*., **1990**, 112, 3068.

50. Perrott, A. L.; Arnold, D. R., *Can. J. Chem.,* **1992**, 70, 272.

51. Maslak, P.; Asel, S. L., *J. Am. Chem. Soc*., **1988**, 110, 8260.

52. Maslak, P.; Chapman, Jr., W. H., *J. Chem. Soc. Chem. Commun.* **1989**, 1809.

53. Maslak, P.; Chapman, Jr., W. H., *Tetrahedron*, 1990, 46, 2715.

54. Maslak, P.; Chapman, Jr., W. H.; Vallombroso, Jr., T. M.; Watson, B. A., *J. Am. Chem. Soc*., 1995, 117, 12380.

55. Maslak, P.; Chapman, Jr., W. H., *J. Org. Chem*., 1996, 61, 2647.

56. Rehm, D.; Weller, A., *Isr. J. Chem.*, **1970**, *8*, 259.

57. This estimate is based on the fact that both aryl rings in the β-1 models are 1-alkyl-3,4-dimethoxy substituted.

58. Wayner, D. D. M.; McPhee, D. J.; Griller, D., *J. Am. Chem. Soc.*, **1988**, 110, 132.

59. Sim, B. A., Milne; P. H. Griller, D.; Wayner, D. D. M., *J. Am. Chem. Soc*., **1990**,112, 6635.

60. Wayner, D. D. M.; Sim. B. A.; Dannenberg, J.J., *J. Org. Chem*., **1991**, 56, 4853.

61. Bonini, C.; D'Auria, M. D.; D'Alessio, L. D.; Mauriello, G.; Tofani, D.; Viggiano, D.; Zimbardi, F., *J. Photochem. and Photobiol. A*, **1998**, 113, 119.

62. Bonini, C.; D'Auria, M. D.; D'Alessio, L. D.; Mauriello, G.; Tofani, D.; Viggiano, D.; Zimbardi, F., *J. Photochem. and Photobiol. A*, **1998**, 118, 107.

63. Bentivenga, G.; Bonini, C.; D'Auria, M.; De Bona, A.; Mauriello, G., *Chemosphere*, **1999**, 14, 2409.

64. Bentivenga, G.; Bonini, C.; D'Auria, M.; De Bona, A., *J. Photochem. and Photobiol. A*, **1999**, 128, 139.

65. Crestini, C.; D'Auria, M., *Tetrahedron*, **1997**, *53*, 7877.

66. McNally, A. M.; Moody, E. C.; McNeill, K., *Photochem. Photobiol. Sci.,* **2005**, *4*, 268.

67. Eriksen, J.; Foote, C. S., *J. Am. Chem. Soc.*, **1980**, *102*, 6083.

68. Kojima, M.; Kuriyama, Y.; Sakuragi, H.; Tokumaru, K., *Bull. Chem. Soc. Jpn.*, **1991**, *64*, 2724.

69. Chandross, E. A.; Ferguson, J., *J. Chem. Phys.* **1967**, *47*, 2557.

70. Sheldon, R. A.; Kochi. J. K. *Metal Catalyzed Oxidations of Organic Compounds*, **1981**, Academic Press, NY.

71. This prediction is based on the fact that the C1-aryl ring is 1-alkyl-3,4-

dialkoxy substituted whereas the C2-aryl ring is 1,2-dialkoxy substituted.

72. Grenier, J-L.; Catteau, J-P.; Cotelle, P., *Syn. Commun.*, **1999**, *29*, 1201.

73. Bohlin, C.; Anderson, P-O.; Lundquist, K.; Jönsson, L., *J. Mole. Cat. B*, **2007**, 45, 21.

74. Bohlin, C.; Lundquist, K.; Jönsson, L., *J. Enzyme and Microbial Tech*., **2008**, 43,199.

75. Bohlin, C.; Lundquist, K.; Jönsson, L. *J. Bioorg. Chem*., **2009**, 37, 143.

76. Rochefort, D.; Bourbonnais, R.; Leech, D.; Paice, M. G. *Chem. Commun*., **2002**, 1182.

77. Camaioni, D. M., *J. Am. Chem. Soc.*, **1990**, *112*, 9475.

78. Beste, A.; Buchanan III, A. C., *J. Org. Chem*., **2009**, 74, 2837.

79. Wariishi, H.; Sheng, D.; Gold, M. H., *Biochemistry*, **1994**, 33, 5545-5552

80. Srebotnik, E.; Hammel, K. E. *J. Biotech.*, **2000**, *81*, 179; Vicario, J. L.; Badia, D.; Carillo, L. *Tetrahedron*, **2003**, *14*, 489.